Trends in Renewable Energy
OPEN ACCESS ISSN: 2376-2144
Peer-Reviewed Article futureenergysp.com/index.php/tre

Power Systems Stability through Piecewise Monotonic Data Approximations – Part 1: Comparative Benchmarking of L1PMA, L2WPMA and L2CXCV in Overhead Medium-Voltage Broadband over Power Lines Networks

Athanasios G. Lazaropoulos*

School of Electrical and Computer Engineering / National Technical University of Athens / 9 IroonPolytechniou Street / Zografou, GR 15780

Received October 20,2016; Accepted November 11, 2016; Published January 1, 2017

This first paper assesses the performance of three well-known piecewise monotonic data approximations (*i.e.*, L1PMA, L2WPMA, and L2CXCV) during the mitigation of measurement differences in the overhead medium-voltage broadband over power lines (OV MV BPL) transfer functions.

The contribution of this paper is triple. First, based on the inherent piecewise monotonicity of OV MV BPL transfer functions, L2WPMA and L2CXCV are outlined and applied during the determination of theoretical and measured OV MVBPL transfer functions. Second, L1PMA, L2WPMA, and L2CXCV are comparatively benchmarked by using the performance metrics of the percent error sum (PES) and fault PES. PES and fault PES assess the efficiency and accuracy of the three piecewise monotonic data approximations during the determination of transmission BPL transfer functions. Third, the performance of L1PMA, L2WPMA, and L2CXCV is assessed with respect to the nature of faults —*i.e.* faults that follow either continuous uniform distribution (CUD) or normal distribution (ND) of different magnitudes—.

The goal of this set of two papers is the establishment of a more effective identification and restoration of the measurement differences during the OV MV BPL coupling transfer function determination that may significantly help towards a more stable and self-healing power system.

Keywords: Smart Grid; Intelligent Energy Systems; Broadband over Power Lines (BPL) networks; Power Line Communications (PLC); Faults; Fault Analysis; Fault Identification and Prediction; Power System Stability; Distribution Power Grids

1. Introduction

In recent years, the broadband over powerlines (BPL) technology has attracted significant popularity as a connectivity solution in homes and a provider of various smart grid related applications [1]. More specifically, the deployment of BPL networks across the vintage transmission and distribution power grids transforms them into an intelligent IP-based communications network further enhancing power system stability [2], [3]. Among the characteristics of this communications network, its low-cost deployment and potential of broadband last mile access through its wired/wireless interfaces render the

*Corresponding author: AGLazaropoulos@gmail.com

Tr Ren Energy, 2017, Vol.3, No.1, 2-32. doi: 10.17737/tre.2017.3.1.0029

BPL technology both as a useful power grid complement and a strong telecommunications competitor to wireless networking solutions [4].

Thanks to the HomePlug Powerline Alliance, which is leading the standardization process of the BPL technology, more than 100 million BPL devices with an annual growth rate of 30% have already been deployed and are able to deliver high-bandwidth applications (e.g., HD video streaming and VoIP) with data rates that exceed 1Gbps [5]-[7]. To achieve these data rates, various inherent BPL deficiencies, such as high and frequency-selective channel attenuation and noise, should be overcome [8]-[13].

As the determination of the transfer functions of overhead medium-voltage (OV MV) BPL networks is concerned in this paper, the well-established hybrid method, which is employed to examine the behavior of various multiconductor transmission line (MTL) structures, is also adopted in this paper [2], [8]-[12], [14]-[25]. Given the OV MV BPL network topology, OV MV MTL configuration, and the applied coupling scheme as inputs, the hybrid method gives as an output the corresponding transfer function.

Despite the theoretical accuracy of the hybrid method during the determination of OV MV BPL transfer functions, a number of practical reasons and "real-life" conditions may create measurement differences between experimental and theoretical results. On the basis of six measurement difference categories, which are analyzed in [2], [24], [25], OV MV BPL transfer functions are significantly distorted critically affecting the monitoring and surveillance of the distribution power grid. To mitigate the aforementioned measurement differences and restore the undistorted OV MV BPL transfer function, a piecewise monotonic data approximation is applied [26]-[33]. Until now, only L1PMA has been applied and examined in transmission and distribution BPL networks [2], [24], [25]. Here, another two piecewise monotonic data approximations by Demetriou are first applied and comparatively benchmarked in comparison with the already validated L1PMA; say, L2WPMA [34] and L2CXCV [35].

The rest of this paper is organized as follows: In Sec. II, the OV MV MTL configuration and the respective indicative OV MV BPL topologies are presented. Sec. III synopsizes the principles of BPL signal propagation and transmission across OV MV BPL topologies. In Sec. IV, a brief presentation of the L1PMA is given. Also, L2WPMA and L2CXCV are analytically outlined. In the same Section, the percent error sum (PES) and fault PES, which are applied in order to benchmark L1PMA, L2WPMA, and L2CXCV, are reported. Sec. V discusses the simulations of various OV MV BPL networks intending to mark out the efficiency of L1PMA, L2WPMA, and L2CXCV and to mitigate the occurred measurement differences. Sec.VI concludes this paper.

2. Distribution Power Grids

2.1 OV MV MTL Configuration

The overhead MV distribution lines, which are examined in this paper, are shown in Fig. 1(a) of [2]. Overhead MV distribution line consists of:

- *Phase lines*: These lines with radii $r_{MV,p}$ are hung at typical heights h_{MV} above ground. The three phase conductors of the OV MV MTL configuration are further spaced by Δ_{MV}.
- *Neutral conductors*: There are no neutral conductors in the examined OV MV MTL configuration.

As regards the overhead MV distribution line configuration, it consists of ACSR three-phase conductors [8], [9], [17]. Exact values concerning conductor properties and configuration geometries are reported in [19].

In accordance with [21], [36]-[38], the ground with conductivity σ_g=5mS/m and relative permittivity ε_{rg}=13 is considered as the reference conductor. The aforementioned ground parameters define a realistic scenario during the following analysis while the impact of imperfect ground on broadband signal propagation via OV MV power lines was analyzed in [8], [9], [17], [19], [21], [39]-[41].

2.2 Indicative OV MV BPL Topologies

In accordance with [8]-[12], [14]-[22], [36], [42]-[44] and with reference to Fig. 1, average path lengths of the order of 1,000m are considered in OV MV BPL topologies. Hence, the following four indicative OV MV BPL topologies, concerning end-to-end connections of average path lengths, are examined, namely:

1. A typical urban topology (OV MV urban case) with N=3 branches (L_1=500m, L_2=200m, L_3=100m, L_4=200m, L_{b1}=8m, L_{b2}=13m, L_{b3}=10m).
2. A typical suburban topology (OV MV suburban case) with N=2 branches (L_1=500m, L_2=400m, L_3=100m, L_{b1}=50m, L_{b2}=10m).
3. A typical rural topology (OV MV rural case) with only N=1 branch (L_1=600m, L_2=400m, L_{b1}=300m).
4. The "LOS" transmission along the same end-to-end distance $L=L_1+\ldots+L_{N+1}$=1000m when no branches are encountered. This topology corresponds to Line of Sight transmission in wireless channels.

The four indicative OV MV BPL topologies are going to be used so that the accuracy of L1PMA, L2WPMA, and L2CXCV is evaluated in Sec. V.

The assumptions for the circuital parameters of OV MV BPL topologies, which are concerned in this paper, are the same as [2], namely: (i) The branch lines are assumed identical to the transmission ones; (ii) The interconnections between the transmission and branch conductors of the lines are fully activated; (iii) The transmitting and the receiving ends are assumed to match the characteristic impedance of the modal channels; and (iv) The branch terminations are assumed to be open circuits.

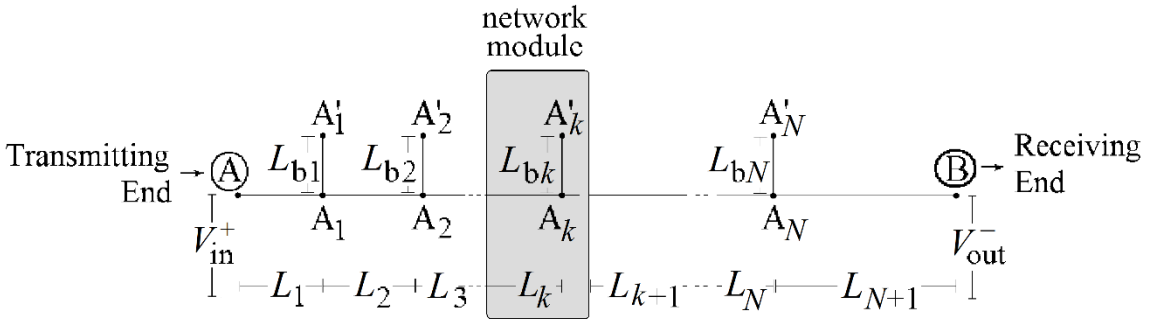

Figure 1. General OV MV BPL topology [2].

3. A Briefing of BPL Propagation and Transmission Analysis

3.1 Hybrid Method and Channel Transfer Function

The well-established hybrid method, which has been tested successfully in various transmission and distribution BPL networks [8]-[12], [14]-[23], [40]-[42], is also applied in this paper. Consisting of: (i) a bottom-up approach that is based on the MTL theory, eigenvalue decomposition (EVD), and singular value decomposition (SVD); and (ii) a top-down approach that is denoted as TM2 method and based on the concatenation of multidimensional chain scattering matrices, the hybrid method gives as an output the corresponding transfer function when the OV MV BPL network topology, OV MV MTL configuration and the applied coupling scheme are given as inputs.

3.2 MTL Theory, EVD and Channel Transfer Functions

As it has already been mentioned in [8]-[12], [14]-[18], [21], [36], the standard TL analysis can be extended to the MTL case through a matrix approach. Since the n^{OVMV}+1 conductors of the OV MV MTL configuration are laid parallel to the z axis, n^{OVMV} modes are supported by the MTL configuration. Through TM2 method, their spectral behavior is described by the $n^{\mathrm{OVMV}} \times n^{\mathrm{OVMV}}$ EVD modal transfer function matrix $\mathbf{H}^{\mathrm{m}}\{\cdot\}$ whose elements $H_{i,j}^{\mathrm{m}}\{\cdot\}$, $i, j = 1,\ldots,n^{\mathrm{OVMV}}$ are the EVD modal transfer functions where $H_{i,j}^{\mathrm{m}}$ denotes the element of matrix $\mathbf{H}^{\mathrm{m}}\{\cdot\}$ in row *i* of column *j*.

Since the EVD modal transfer function matrix is already evaluated, the $n^{\mathrm{OVMV}} \times n^{\mathrm{OVMV}}$ channel transfer function matrix $\mathbf{H}\{\cdot\}$ is determined by

$$\mathbf{H}\{\cdot\} = \mathbf{T}_V \cdot \mathbf{H}^m\{\cdot\} \cdot \mathbf{T}_V^{-1} \tag{1}$$

where $\mathbf{T}_V$ is a $n^{\mathrm{OVMV}} \times n^{\mathrm{OVMV}}$ matrix that depends on the frequency, the OV MV MTL configuration and the physical properties of the cables [8]-[12], [14]-[18], [21], [36], [45].

3.3 Coupling Schemes and Coupling Transfer Functions

According to how signals are injected into OV MV lines, two categories of coupling schemes are mainly supported by the OV MV BPL networks, namely [2], [16], [18], [24], [25], [46]-[48]: (i) Wire-to-Ground (WtG) coupling schemes; and (ii) Wire-to-Wire (WtW) coupling schemes. Since the main interest of this paper is the comparative benchmark of the piecewise approximation methods, only one of the previous coupling schemes is going to be applied in the following analysis for the sake of clarity and terseness; say, WtG coupling scheme.

In the case of WtG coupling schemes, the coupling WtG channel transfer function $H^{\mathrm{WtG^s}}\{\cdot\}$ is given from

$$H^{\mathrm{WtG^s}}\{\cdot\} = \left[\mathbf{C}^{\mathrm{WtG}}\right]^{\mathrm{T}} \cdot \mathbf{T}_V \cdot \mathbf{H}^m\{\cdot\} \cdot \mathbf{T}_V^{-1} \cdot \mathbf{C}^{\mathrm{WtG}} \tag{2}$$

where $\mathbf{C}^{\mathrm{WtG}}$ is a 3×1 coupling column vector with zero elements except in row *s* where the value is equal to 1. Note that WtG coupling schemes inject the signal onto the conductors, *s*=1,...,3 while the signal returns via the ground. WtG coupling between conductor *s* and ground will be denoted as WtG^s, hereafter.

4. Presentation of L1PMA, L2WPMA, and L2CXCV

4.1 Introduction to Piecewise Monotonic Data Approximation Methods of Demetriou

Similarly to L1PMA, various monotonic data approximation methods have been proposed by Demetriou, such as L2WPMA and L2CXCV. Their application, which is theoretically presented and experimentally verified in [2], [24]-[31], successfully copes with problems that are derived from the presence of measurement differences during the OV MV BPL transfer function determination. Until now, only the efficiency of the best L1PMA to mitigate measurement differences during the determination of OV MV BPL transfer functions has been assessed [2], [24], [25]. In this paper, L2WPMA and L2CXCV are comparatively benchmarked against L1PMA when the mitigation of the occurred measurement differences during the OV MV BPL transfer function determination is required.

4.2 L1PMA

L1PMA exploits the piecewise monotonicity property that always occurs in transmission and distribution BPL transfer functions [2], [24], [25]. Actually, L1PMA decomposes the BPL transfer function into separate monotonous sections between its adjacent turning points (primary extrema) [28], [29]. Since the separate monotonous sections are identified, L1PMA separately handles them. On the basis of the minimization of the moduli sum of the measurement differences, L1PMA achieves to mitigate the uncorrelated measurement differences by neglecting the existence of few large ones [2], [49]. A detailed analysis concerning the application of L1PMA to distribution and distribution BPL transfer functions is given in [2], [24], respectively.

Apart from its sound theoretical background, another strong point of L1PMA is its easy and online software availability. In fact, the Fortran software package that is applied to implement the L1PMA has extensively been verified in various scientific fields [29], [31], [50]-[52] and is freely available online in [53]. In general terms, L1PMA software receives as inputs the measured OV MV BPL coupling transfer function, the measurement frequencies and the number of monotonic sections (*i.e.*, either user- or computer-defined) and gives as outputs the optimal primary extrema and the best fit of the measured OV MV BPL coupling transfer function.

4.3 L2WPMA

In accordance with [34], L2WPMA decomposes the examined BPL transfer function, which is contaminated by measurement differences, into separate monotonous sections between its primary extrema. Then, L2WPMA minimizes the weighted sum of the square of the measurement differences by requiring specific number of sign changes in the first divided measurement differences of the approximation. The number of sign changes is equal to the number of monotonic sections minus one where the number of monotonic sections is either user- or computer-defined.

Similarly to L1PMA, the Fortran software package that is applied to implement L2WMPA is freely available online in [34]. In fact, Fortran software employs a dynamic programming technique that divides the BPL transfer function data into disjoint sets of adjacent data and solves a problem of monotonic fit or isotonic regression for each set. The number of disjoint sets is at most equal to the defined number of monotonic sections. In comparison with the Fortran software of L1PMA, L2WPMA is characterized by

shorter computation times due to its lower complexity. In general terms, L2WPMA software receives the same inputs with the L1PMA one and gives as outputs a spline representation of the solution, the corresponding Lagrange multipliers and the best fit of the measured OV MV BPL coupling transfer function.

4.4 L2CXCV

In accordance with [35], L2CXCV smooths the OV MV transfer function data (in the least square error sense), which are contaminated with measurement differences. In fact, L2CXCV smoothing is subject to one sign change in the second divided differences of the smoothed values. In contrast with L1PMA and L2WPMA, the number of monotonic sections is neither user- nor computer-defined since L2CXCV partitions the data into two disjoint sets of adjacent data and calculates the required fit by solving a strictly convex quadratic programming problem for each set. The quadratic programming technique makes use of active sets and takes advantage of a B-spline representation of the smoothed values [35].

Similarly to L1PMA and L2WPMA, the entire Fortran code that is required to implement L2CXCV is freely available online in [54]. In general, L2CXCV receives as input the measured OV MV BPL coupling transfer function and gives as output the fit of the measured OV MV BPL coupling transfer function.

4.5 The Nature of Measurement Differences and the Mathematics of Piecewise Monotonic Data Approximation Methods

As already been mentioned, a set of practical reasons and "real-life" conditions create significant differences between experimental measurements and theoretical results during the transfer function determination of BPL networks. The reasons for these measurement differences can be grouped into six categories that are analytically reported in [2], [24], [25], [55]-[57]. The measured OV MV BPL coupling transfer function $\overline{H^{\mathrm{WtG}}}\{\cdot\}$ is then determined by

$$\overline{H^{\mathrm{WtG}}}(f_i) = H^{\mathrm{WtG}}(f_i) + e(f_i),\ i=1,\ldots,u \tag{3}$$

where $f_i, i=1,\ldots,u$ denotes the measurement frequency, $e(f_i)$ synopsizes the total measurement difference due to the aforementioned six categories and u is the number of subchannels in the examined frequency range.

Generalizing eq. (3), the measured OV MVBPL coupling transfer function column vector $\overline{\mathbf{H}^{\mathrm{WtG}}}$ is then determined by

$$\overline{\mathbf{H}^{\mathrm{WtG}}} \equiv \overline{\mathbf{H}^{\mathrm{WtG}}}(\mathbf{f}) = \left[\overline{H^{\mathrm{WtG}}}(f_1) \quad \cdots \quad \overline{H^{\mathrm{WtG}}}(f_i) \quad \cdots \quad \overline{H^{\mathrm{WtG}}}(f_u)\right]^{\mathrm{T}} \tag{3}$$

where $\mathbf{f} = \left[f_1 \quad \cdots \quad f_i \quad \cdots \quad f_u\right]^{\mathrm{T}}$ is the measurement frequency column vector and f_i, $i=1,\ldots,u$ are the measurement frequencies. Similarly to the measured OV MV BPL coupling transfer function column vector $\overline{\mathbf{H}^{\mathrm{WtG}}}$, the theoretical OV MV BPL coupling transfer function column vector $\mathbf{H}^{\mathrm{WtG}}$ can also be defined.

With reference to Secs. IV B-D, the measured OV MV BPL coupling transfer function column vector, the measurement frequency column vector and the number of monotonic sections (only for L1PMA and L2WPMA) are received by the three examined piecewise monotonic data approximation methods. With reference to Secs. IV B-D, each monotonic data approximation methods processes its inputs and gives as output the

approximated OV MV BPL coupling transfer function column vector $\overline{\overline{\mathbf{H}^{\mathrm{WtG}}}}(\mathbf{f})$ by applying its algorithm.

4.6 PES and Fault PES for L1PMA, L2WPMA and L2CXCV

As it has already been mentioned in Sec. IV E, to evaluate the approximation accuracy of the piecewise monotonic data approximation methods of this paper and, thus, to comparatively benchmark them, the performance metrics of [2] are used. More specifically, the PES expresses as a percentage the total sum of the relative differences between the approximated coupling transfer function and the theoretical coupling transfer function for all the used frequencies, namely

$$PES = 100\% \cdot \frac{\sum_{i=1}^{u} \left| \overline{\overline{\mathbf{H}^{\mathrm{WtG}}}}(f_i) - \mathbf{H}^{\mathrm{WtG}}(f_i) \right|}{\sum_{i=1}^{u} \left| \mathbf{H}^{\mathrm{WtG}}(f_i) \right|} \tag{4}$$

With respect to eq. (4), to assess the mitigation efficiency of the piecewise monotonic data approximation methods towards the faults, PES is compared against the fault PES that is given by

$$PES_{\text{fault}} = 100\% \cdot \frac{\sum_{i=1}^{u} \left| \overline{\mathbf{H}^{\mathrm{WtG}}}(f_i) - \mathbf{H}^{\mathrm{WtG}}(f_i) \right|}{\sum_{i=1}^{u} \left| \mathbf{H}^{\mathrm{WtG}}(f_i) \right|} \tag{5}$$

5. Numerical Results and Discussion

5.1 Simulation Goals and Parameters

Various topologies of OV MV BPL networks are simulated with the purpose of comparatively benchmarking the approximation efficiency of the piecewise monotonic data approximation methods that are examined in this paper when various faults occur.

As regards the simulation specifications, those are the same with [2], [24], [25]. More specifically, the BPL frequency range and the flat-fading subchannel frequency spacing are assumed equal to 1-30MHz and 1MHz, respectively. Therefore, the number of subchannels in the examined frequency range is equal to 30. Arbitrarily, the WtG^3 coupling scheme is applied during the following simulations. As it is usually done [12], [14], [15], [17], [19], [58], the selection of representative coupling schemes is a typical procedure for the sake of reducing manuscript size.

5.2 Theoretical and Approximated OV MV BPL Transfer Functions by Applying L1PMA, L2WPMA and L2CXCV

Prior to comparatively benchmarking L1PMA, L2WPMA, and L2CXCV, their overall performance against the mitigation of measurement differences during the determination of the OV MV BPL coupling transfer functions is presented in this subsection.

In Figs. 2(a)-(d), the theoretical coupling transfer function is plotted versus frequency for the four indicative OV MV BPL topologies, respectively, when WtG^3

coupling scheme is applied. In each figure, L1PMA result is also plotted for a number of representative monotonic sections (*i.e.*, k_{sect}=2, k_{sect}=5, and k_{sect}=20). In Figs. 3(a)-(d) and Figs. 4(a)-(d), similar curves with Figs. 2(a)-(d) are shown for L2WPMA (same cases of monotonic sections) and L2CXCV (no monotonic sections), respectively.

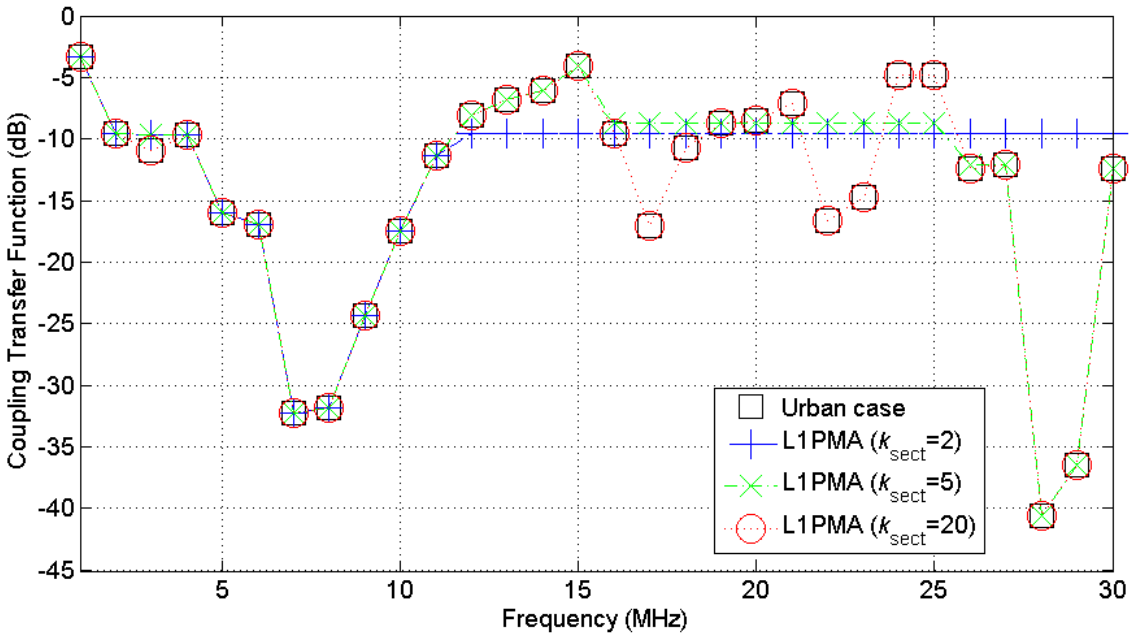

(a)

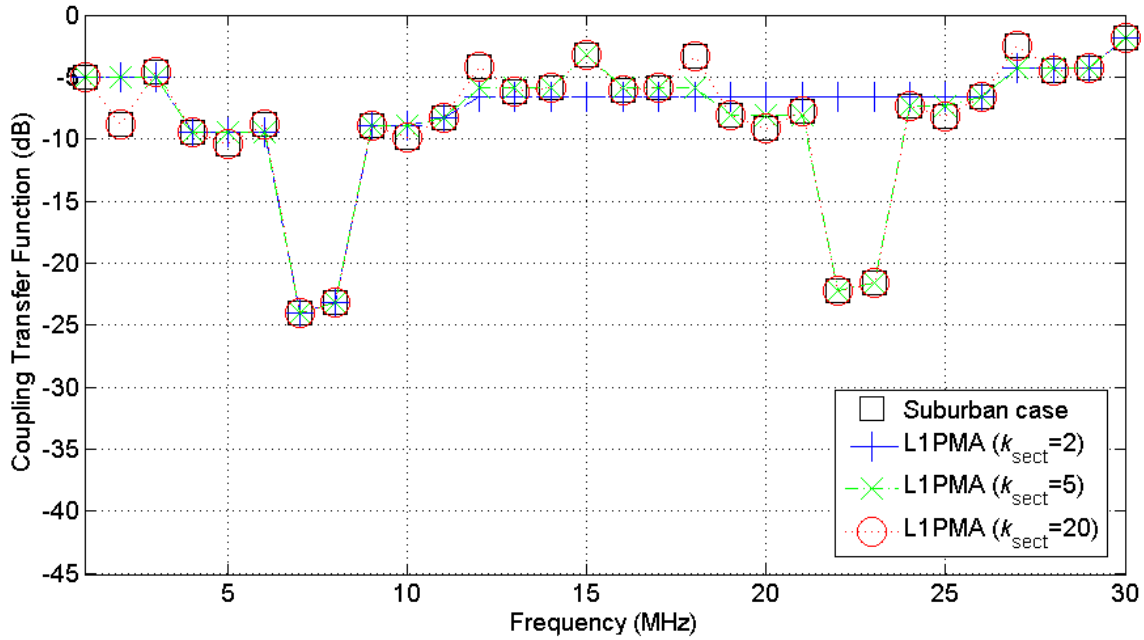

(b)

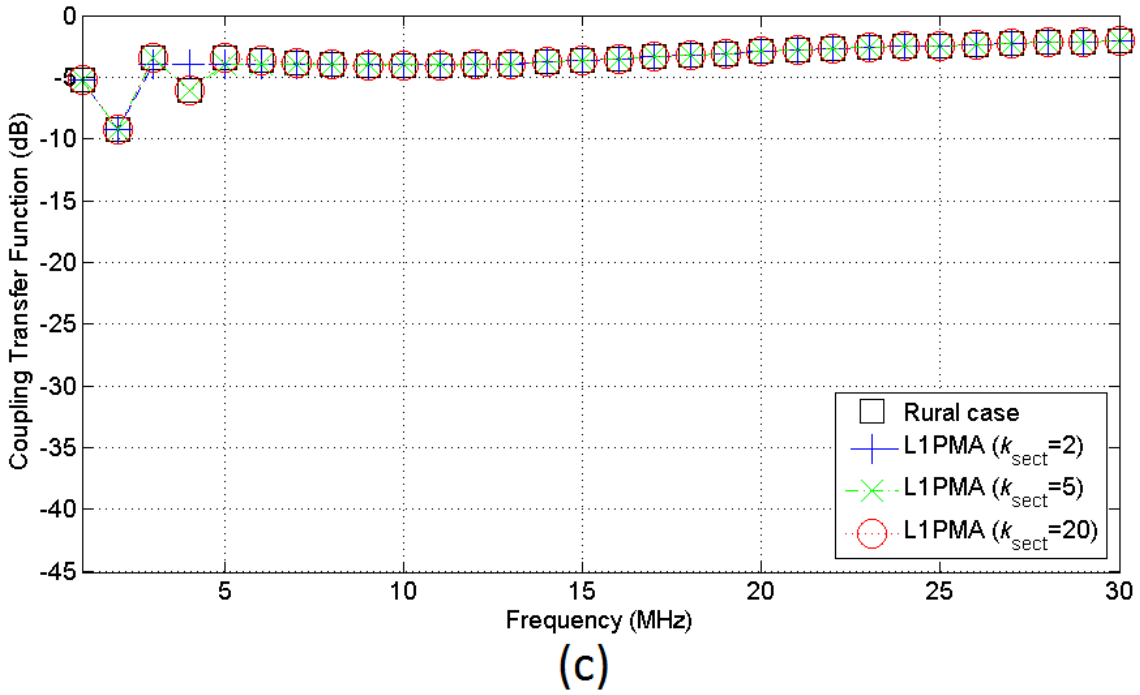

Figure 2. OV MV BPL Coupling transfer function when L1PMA is applied for three representative cases of monotonic sections. (a) Urban case. (b) Suburban case. (c) Rural case. (d) “LOS” case.

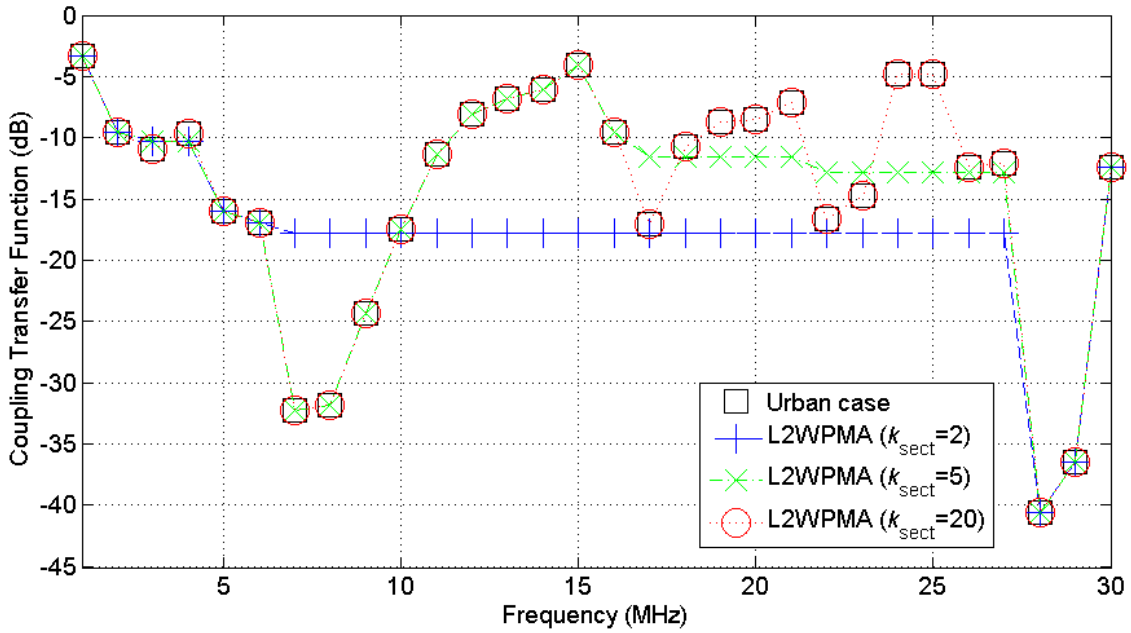
Coupling Transfer Function (dB)
Frequency (MHz)
Urban case
L2WPMA (k_{sect}=2)
L2WPMA (k_{sect}=5)
L2WPMA (k_{sect}=20)

(a)

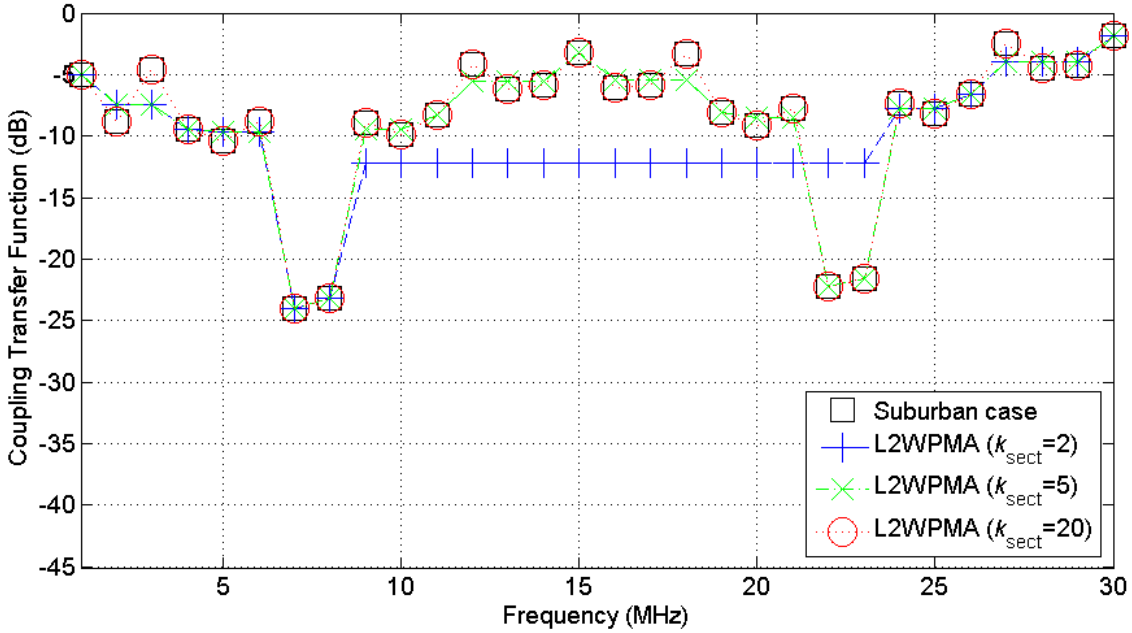
Coupling Transfer Function (dB)
Frequency (MHz)
Suburban case
L2WPMA (k_{sect}=2)
L2WPMA (k_{sect}=5)
L2WPMA (k_{sect}=20)

(b)

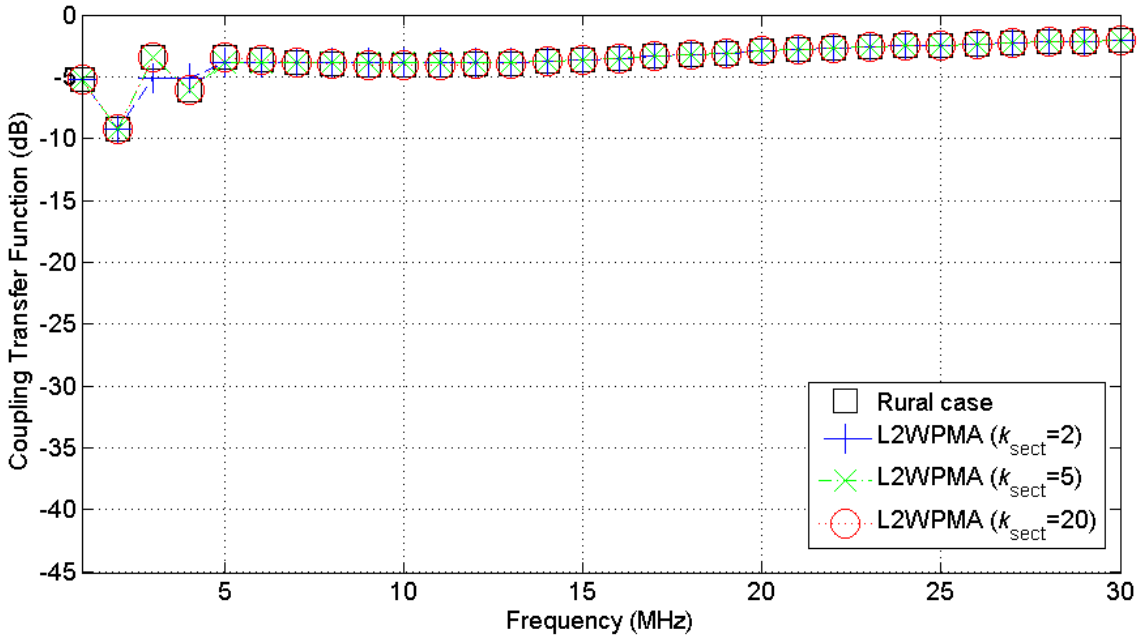

(c)

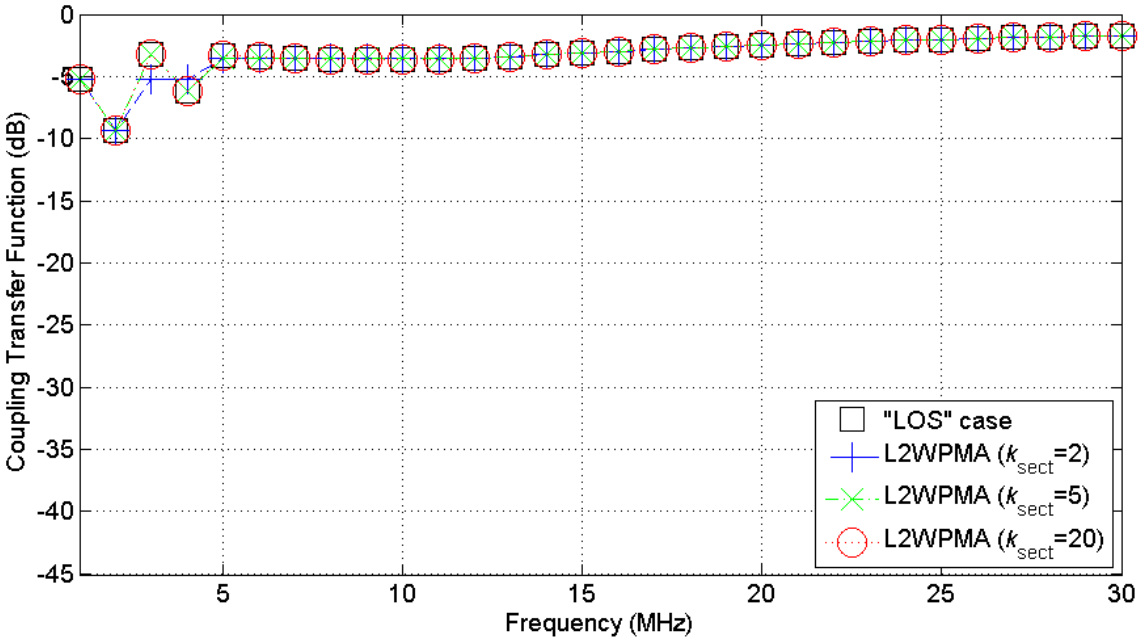

(d)

Figure 3. Same curves with Fig.2 but for L2WPMA for three representative cases of monotonic sections.

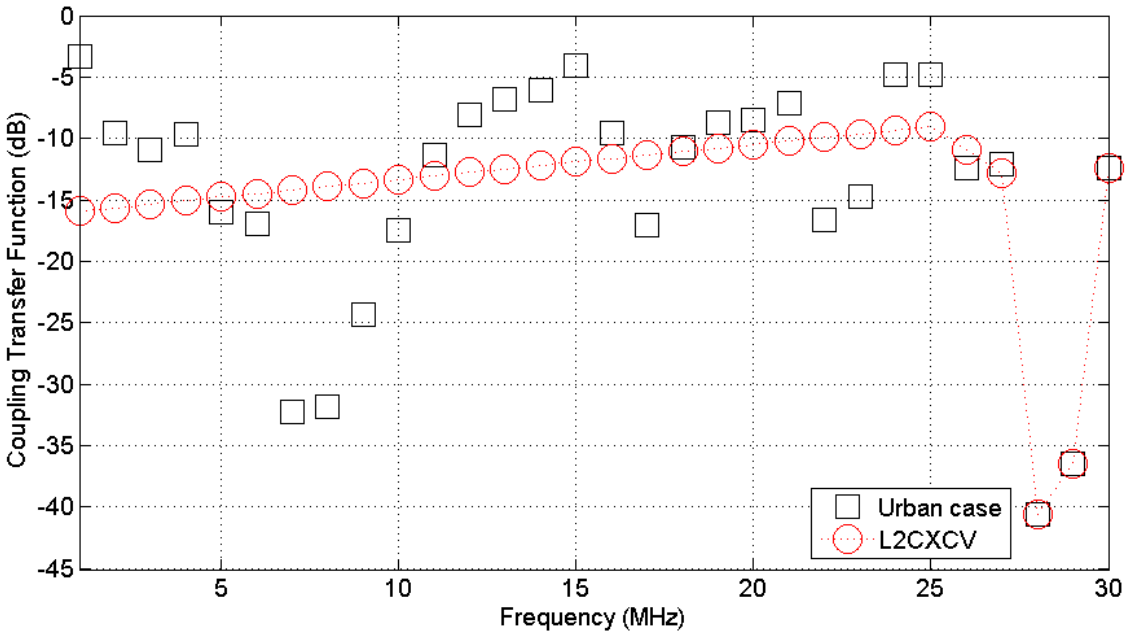
Coupling Transfer Function (dB)
Frequency (MHz)
Urban case
L2CXCV
0
-5
-10
-15
-20
-25
-30
-35
-40
-45
5
10
15
20
25
30

(a)

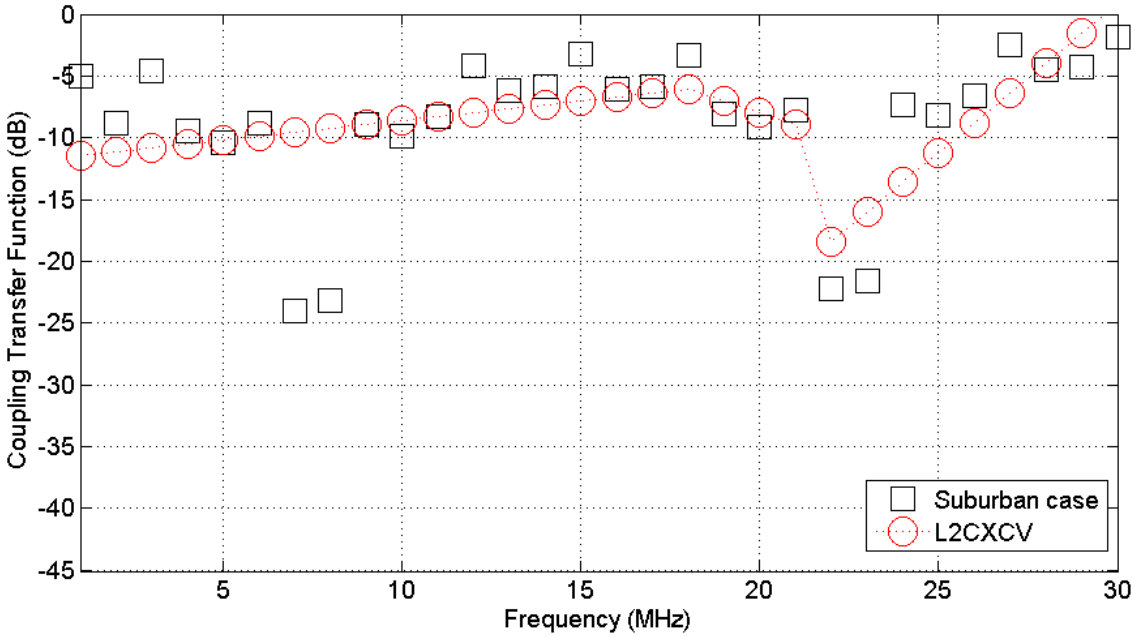
Coupling Transfer Function (dB)
Frequency (MHz)
Suburban case
L2CXCV
0
-5
-10
-15
-20
-25
-30
-35
-40
-45
5
10
15
20
25
30

(b)

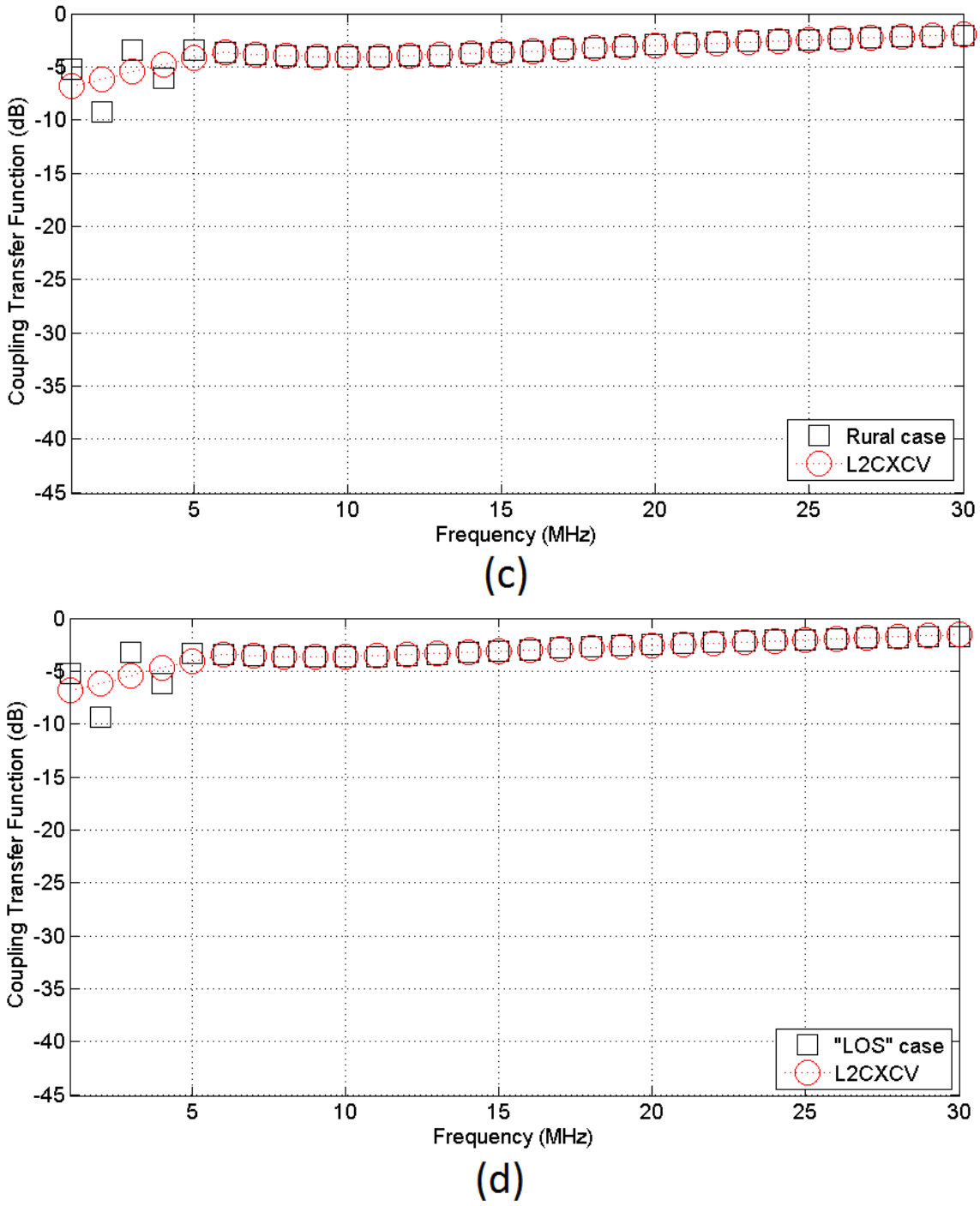

Figure 4. Same curves with Fig.2 but for L2CXCV.

From Figs. 2(a)-(d), 3(a)-(d), and 4(a)-(d), it is evident that L1PMA and L2WPMA very accurately approximate all the examined coupling transfer functions of the indicative OV MV BPL topologies while the number of monotonic sections remains high. As the number of monotonic sections decreases so does the accuracy of the approximation of L1PMA and L2WPMA. When the number of monotonic sections falls below three, all the three piecewise monotonic data approximations (*i.e.*, L1PMA, L2WPMA, and L2CXCV) present comparable results. In fact, if the number of

monotonic sections is equal to one or two, all the piecewise monotonic data approximations tend to approximate the coupling transfer function data closely to the linear approximation.

As it's already been mentioned in [2], the presence of branches along the end-to-end transmission path causes signal reflections, thus, creating a richer multipath environment that adds new spectral notches (extrema) across the coupling transfer function of "LOS" case. The new extrema that appear in the coupling transfer functions of these topologies (i.e., urban case) differ in depth and extent while they require additional monotonic sections so that the approximation may be accurate. Thanks to their adjustable number of monotonic sections, L1PMA and L2WMPA can improve their approximations so that a better accuracy is achieved and these new extrema can be embodied in their approximations –see approximations of k_{sect}=20 of Figs. 2(a) and 3(a). Indeed, not even one coupling transfer function data is outside the L1PMA and L2WPMA approximations of 20 monotonic sections in the two aforementioned figures. Conversely, L2CXCV approximates the coupling transfer function data without the use of monotonic sections having several approximations of low accuracy as a result when OV MV BPL topologies are examined. As a matter of fact, L2CXCV creates a general approximation rather than an approximation that tries to embody all the coupling transfer function data. To assess the performance of L1PMA, L2WPMA, and L2CXCV, their PES is reported in Table 1 for the four indicative OV MV BPL topologies when different numbers of monotonic sections are applied and no measurement differences are assumed.

TABLE 1
PES between Theoretical and Approximated Coupling Transfer Functions when L1PMA, L2WPMA, and L2CXCV Are Applied

Number of Monotonic Sections	PES (%)											
	Urban case			Suburban case			Rural case			"LOS" case		
	L1PMA	L2WPMA	L2CXCV	L1PMA	L2WPMA	L2CXCV	L1PMA	L2WPMA	L2CXCV	L1PMA	L2WPMA	L2CXCV
1	37.53	48.02	34.55	44.10	74.16	36.64	24.68	30.54	9.45	29.51	40.74	11.39
2	27.06	41.05	34.55	22.45	38.66	36.64	3.79	3.92	9.45	3.93	3.99	11.39
3	15.14	16.57	34.55	22.45	37.04	36.64	3.79	3.92	9.45	3.93	3.99	11.39
4	8.50	9.60	34.55	6.00	6.44	36.64	1.24	1.36	9.45	0.77	0.83	11.39
5	8.50	9.60	34.55	6.00	6.44	36.64	1.24	1.36	9.45	0.77	0.83	11.39
6	3.37	4.26	34.55	4.38	4.81	36.64	7.36×10^{-6}	7.47×10^{-6}	9.45	7.37×10^{-6}	7.59×10^{-6}	11.39
7	3.37	4.26	34.55	4.38	4.81	36.64	7.36×10^{-6}	7.47×10^{-6}	9.45	7.37×10^{-6}	7.59×10^{-6}	11.39
8	0.35	0.35	34.55	3.35	3.59	36.64	7.36×10^{-6}	7.47×10^{-6}	9.45	7.37×10^{-6}	7.59×10^{-6}	11.39
9	0.35	0.35	34.55	3.35	3.59	36.64	7.36×10^{-6}	7.47×10^{-6}	9.45	7.37×10^{-6}	7.59×10^{-6}	11.39
10	0.07	0.07	34.55	2.56	3.01	36.64	7.36×10^{-6}	7.47×10^{-6}	9.45	7.37×10^{-6}	7.59×10^{-6}	11.39
11	0.07	0.07	34.55	2.56	3.01	36.64	7.36×10^{-6}	7.47×10^{-6}	9.45	7.37×10^{-6}	7.59×10^{-6}	11.39
12	1.21×10^{-5}	1.17×10^{-5}	34.55	1.79	2.11	36.64	7.36×10^{-6}	7.47×10^{-6}	9.45	7.37×10^{-6}	7.59×10^{-6}	11.39
13	1.21×10^{-5}	1.17×10^{-5}	34.55	1.79	2.11	36.64	7.36×10^{-6}	7.47×10^{-6}	9.45	7.37×10^{-6}	7.59×10^{-6}	11.39
14	1.21×10^{-5}	1.17×10^{-5}	34.55	1.21	1.57	36.64	7.36×10^{-6}	7.47×10^{-6}	9.45	7.37×10^{-6}	7.59×10^{-6}	11.39
15	1.21×10^{-5}	1.17×10^{-5}	34.55	1.21	1.57	36.64	7.36×10^{-6}	7.47×10^{-6}	9.45	7.37×10^{-6}	7.59×10^{-6}	11.39
16	1.21×10^{-5}	1.17×10^{-5}	34.55	0.67	0.67	36.64	7.36×10^{-6}	7.47×10^{-6}	9.45	7.37×10^{-6}	7.59×10^{-6}	11.39
17	1.21×10^{-5}	1.17×10^{-5}	34.55	0.67	0.67	36.64	7.36×10^{-6}	7.47×10^{-6}	9.45	7.37×10^{-6}	7.59×10^{-6}	11.39
18	1.21×10^{-5}	1.17×10^{-5}	34.55	0.31	0.31	36.64	7.36×10^{-6}	7.47×10^{-6}	9.45	7.37×10^{-6}	7.59×10^{-6}	11.39
19	1.21×10^{-5}	1.17×10^{-5}	34.55	0.31	0.31	36.64	7.36×10^{-6}	7.47×10^{-6}	9.45	7.37×10^{-6}	7.59×10^{-6}	11.39
20	1.21×10^{-5}	1.17×10^{-5}	34.55	7.16×10^{-6}	7.28×10^{-6}	36.64	7.36×10^{-6}	7.47×10^{-6}	9.45	7.37×10^{-6}	7.59×10^{-6}	11.39

The previous remarks concerning Figs. 2(a)-(d), 3(a)-(d), and 4(a)-(d) are reflected on the results of Table 1. Actually, the number of monotonic sections determines the approximation accuracy of L1PMA and L2WPMA to the coupling transfer functions of OV MV BPL networks. In contrast, L2CXCV performance remains stable and relatively poor regardless of the number of monotonic sections since this piecewise data approximation method does not include this property during the computation of its approximation. Further comparing L1PMA and L2WPMA performance, their approximation behavior remains nearly the same when different OV MV BPL topologies are examined and different number of monotonic sections is assumed. Actually, L1PMA presents slightly lower PES results than the respective ones of L2WPMA in the majority of the cases examined.

Already been identified for L1PMA in [2], there is an optimal number of monotonic sections above which the PES improvement remains marginal and uniquely describes the pattern of an OV MV BPL topology. This optimal number mainly depends on the OV MV BPL topology and remains the same either for L1PMA or for L2WPMA. In fact, as the OV MV BPL topology comprises more branches the optimal number of monotonic sections generally increases. From Table 1, the optimal number of monotonic sections is equal to 12, 20, 6, and 6 for the urban, suburban, rural, and "LOS" case, respectively.

On the basis of its identity characteristics, the optimal number of monotonic sections also acts as an efficient countermeasure technique against the measurement differences. Since the optimal number of monotonic sections remains the same for given OV MV BPL topology, the presence of measurement differences can be mitigated for the sake of the preservation of the number of monotonic sections. To validate this concept, the performance of L1PMA, L2WPMA, and L2CXCV is assessed as a measurement difference mitigation technique in the following subsection.

5.3 L1PMA, L2WPMA and L2CXCV against Measurement Differences

In accordance with [2], [24], [25], the six categories of measurement differences can create significant differences between experimental measurements and theoretical results during the determination of OV MV BPL coupling transfer functions. The total measurement difference can be assumed to follow either CUD with minimum value $-\alpha_{CUD}$ and maximum value α_{CUD} or ND with mean μ_{ND} and standard deviation σ_{ND}. Since the conclusions concerning the performance of piecewise monotonic data approximations have been verified to remain almost the same either CUD or ND is applied [2], [25], only one of the previous measurement difference distributions is adopted in the following analysis; say, CUD.

Piecewise monotonic data approximations achieve to mitigate the additive measurement differences by simply maintaining the monotonicity pattern of each OV MV BPL coupling transfer function. To examine the impact of measurement differences on the determination of OV MV BPL coupling transfer functions and the potential of counterbalancing the measurement differences, in Figs. 5(a)-(d), the theoretical and measured coupling transfer functions are plotted versus frequency for the four indicative OV MV BPL topologies, respectively. Note that the measured coupling transfer function corresponds to CUD of α_{CUD}=6dB when the corresponding optimal number of monotonic sections for each OV MV BPL topology is assumed. In each figure, the approximated coupling transfer function of the measured one is also drawn when L1PMA is applied.

In Figs. 6(a)-(d) and 7(a)-(d), same plots are given with Figs. 5(a)-(d) but for the application of L2WPMA and L2CXCV, respectively.

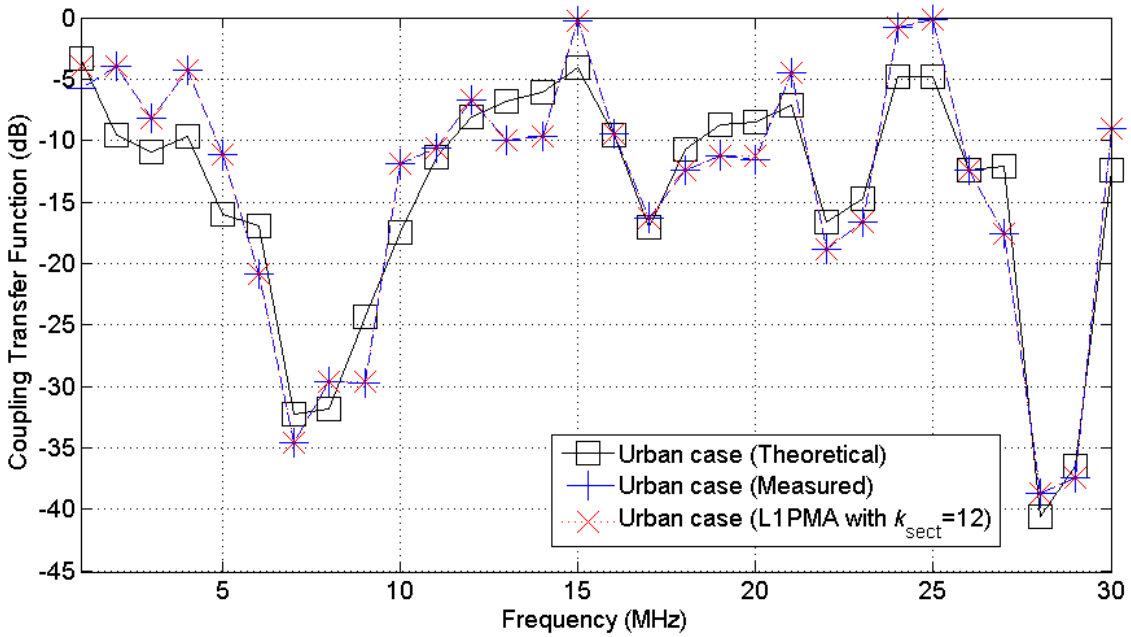

(a)

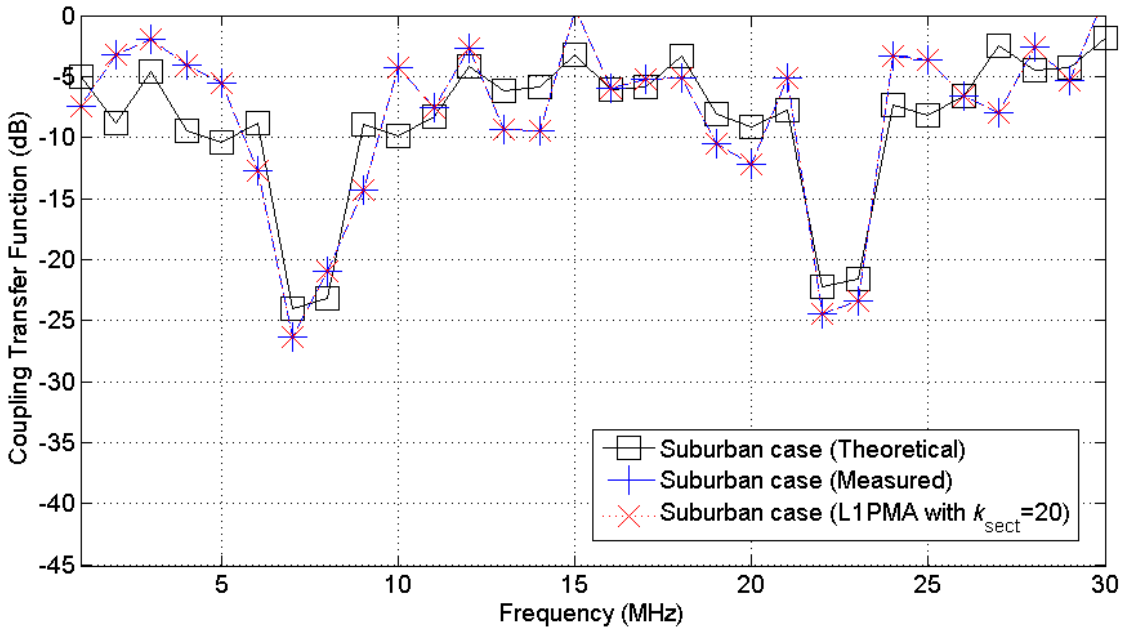

(b)

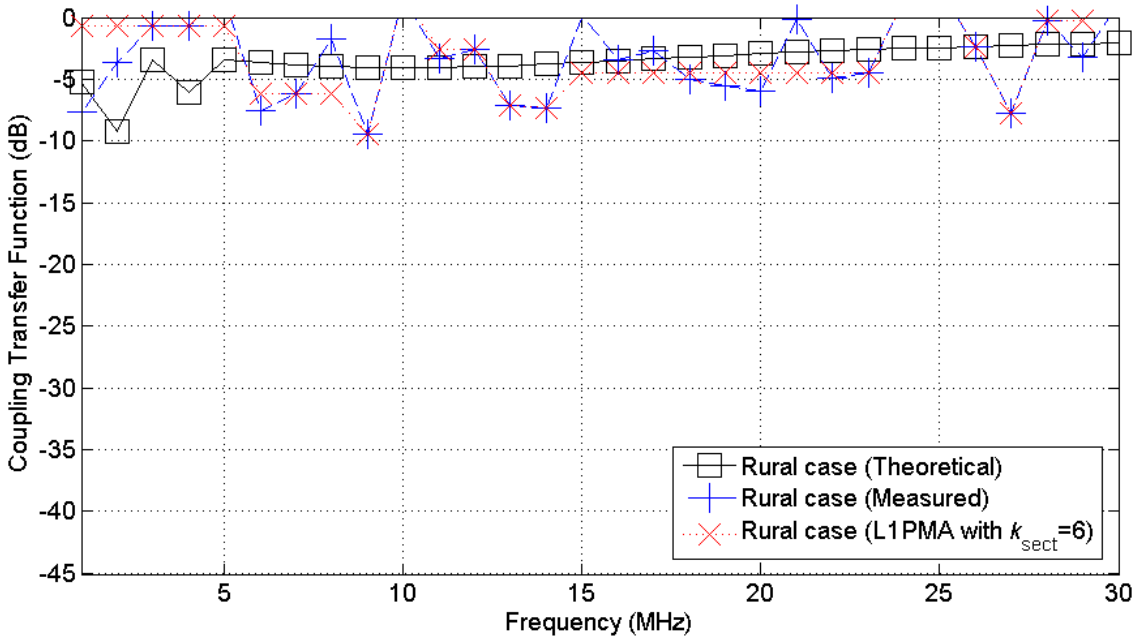

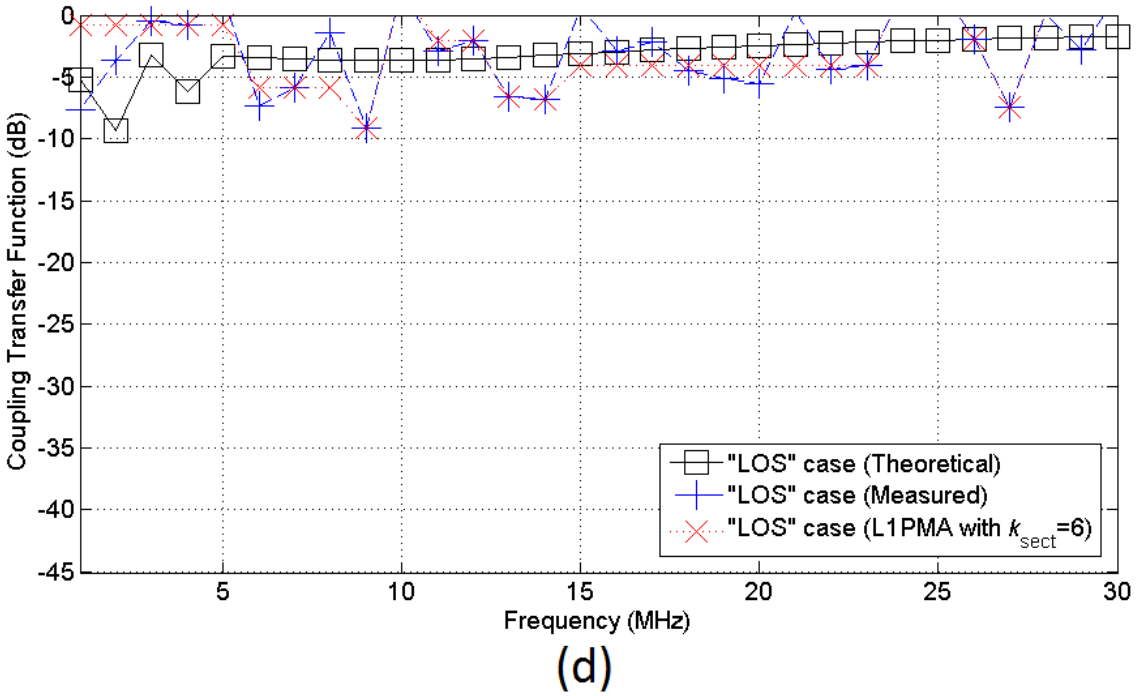

Figure 5. Theoretical, measured, and approximated OV MV BPL coupling transfer function when L1PMA is applied for the indicative measurement difference CUD ofα_{CUD}=6dB. (a) Urban case –the optimal number of monotonic sections is equal to 12–. (b) Suburban case –the optimal number of monotonic sections is equal to 20–. (c) Rural case –the optimal number of monotonic sections is equal to 6–. (d) "LOS" case –the optimal number of monotonic sections is equal to 6–.

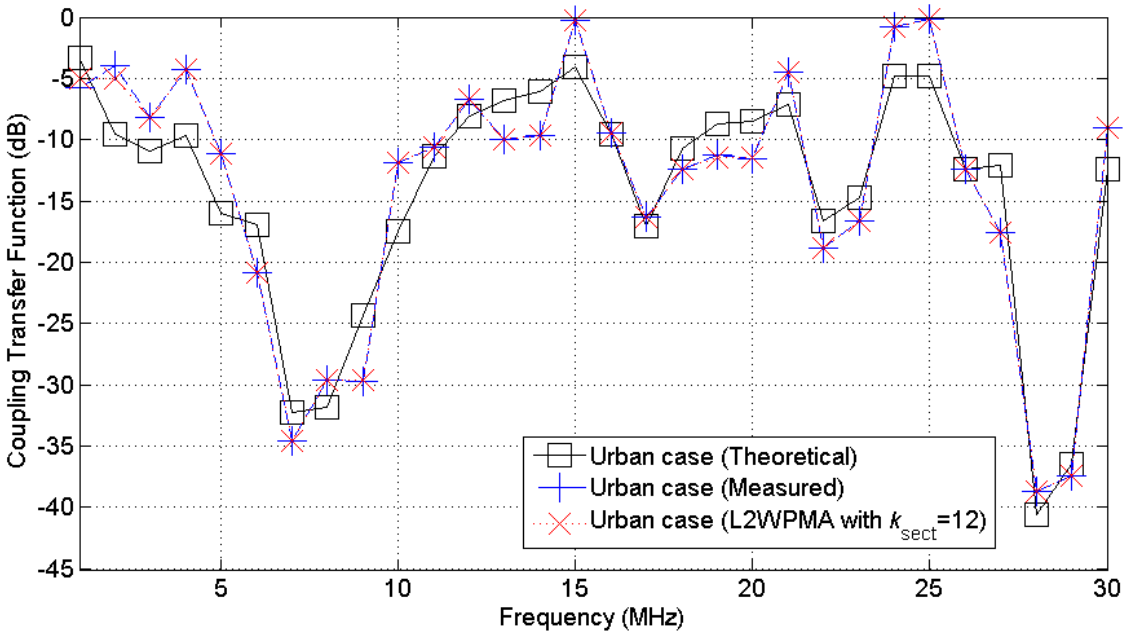
Coupling Transfer Function (dB)
Frequency (MHz)
Urban case (Theoretical)
Urban case (Measured)
Urban case (L2WPMA with k_{sect}=12)

(a)

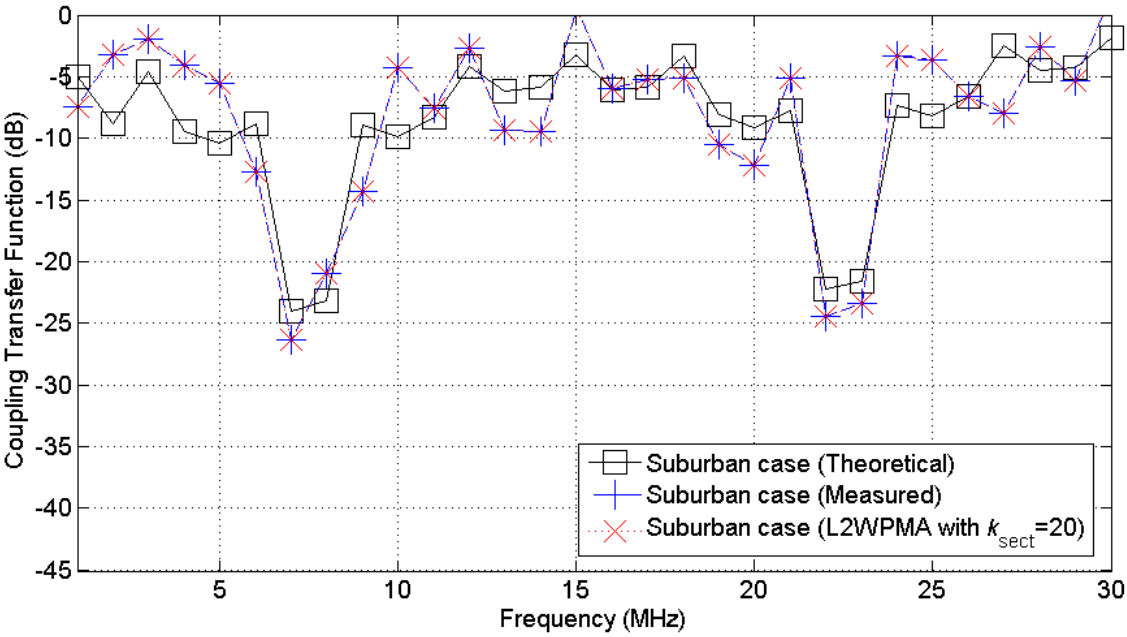
Coupling Transfer Function (dB)
Frequency (MHz)
Suburban case (Theoretical)
Suburban case (Measured)
Suburban case (L2WPMA with k_{sect}=20)

(b)

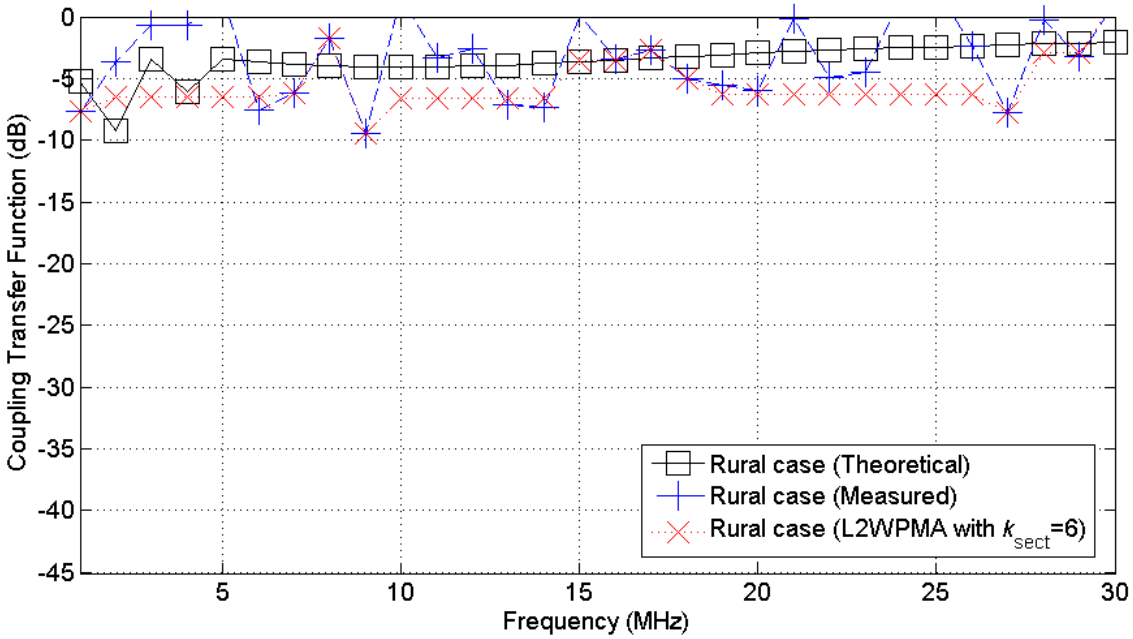

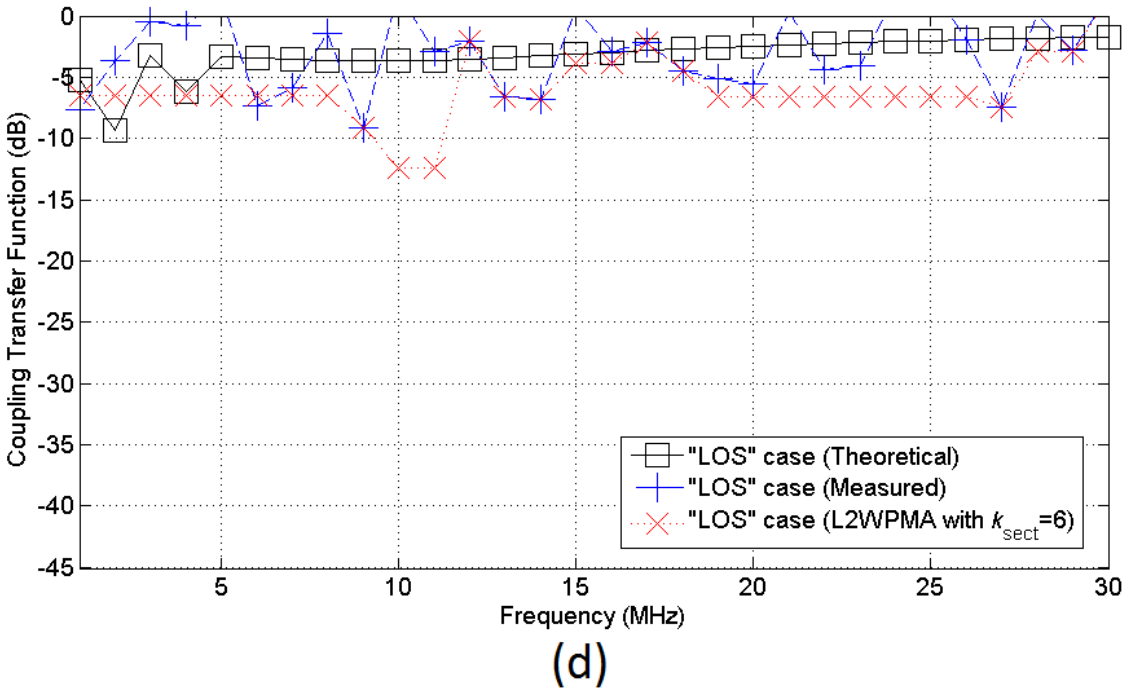

Figure 6. Same curves with Fig.5 but for L2WPMA.

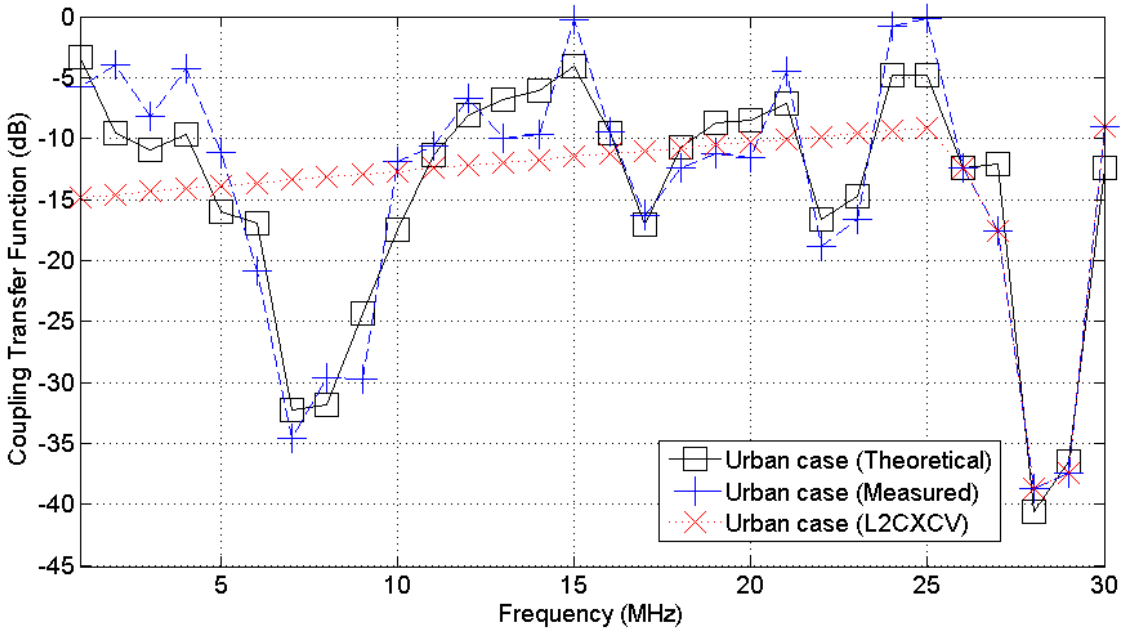
Coupling Transfer Function (dB)
Frequency (MHz)
Urban case (Theoretical)
Urban case (Measured)
Urban case (L2CXCV)

(a)

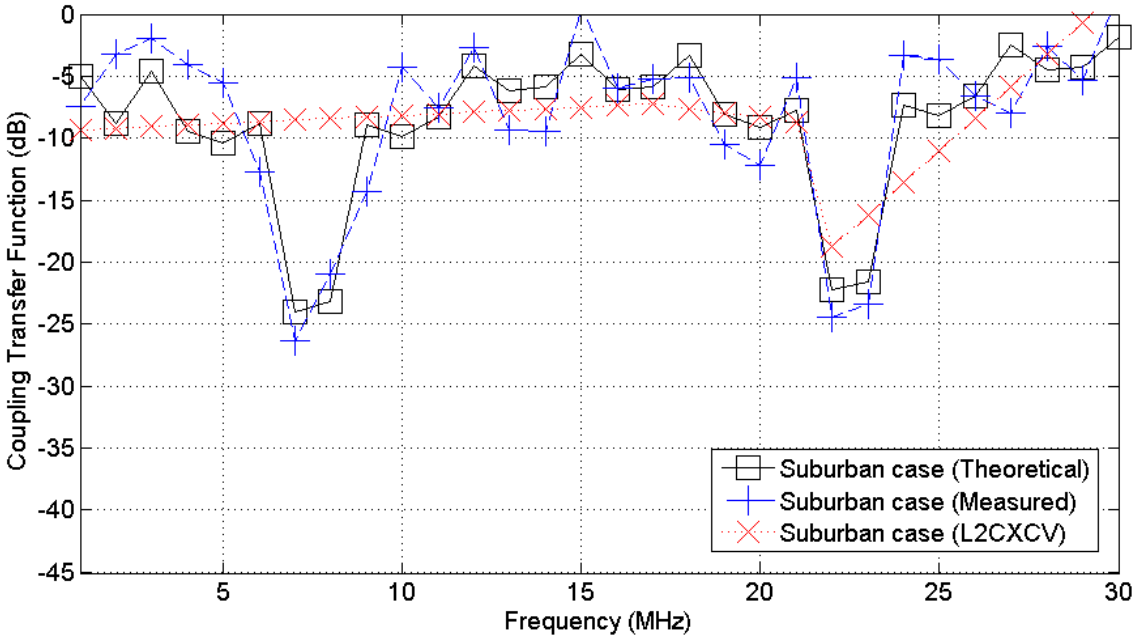
Coupling Transfer Function (dB)
Frequency (MHz)
Suburban case (Theoretical)
Suburban case (Measured)
Suburban case (L2CXCV)

(b)

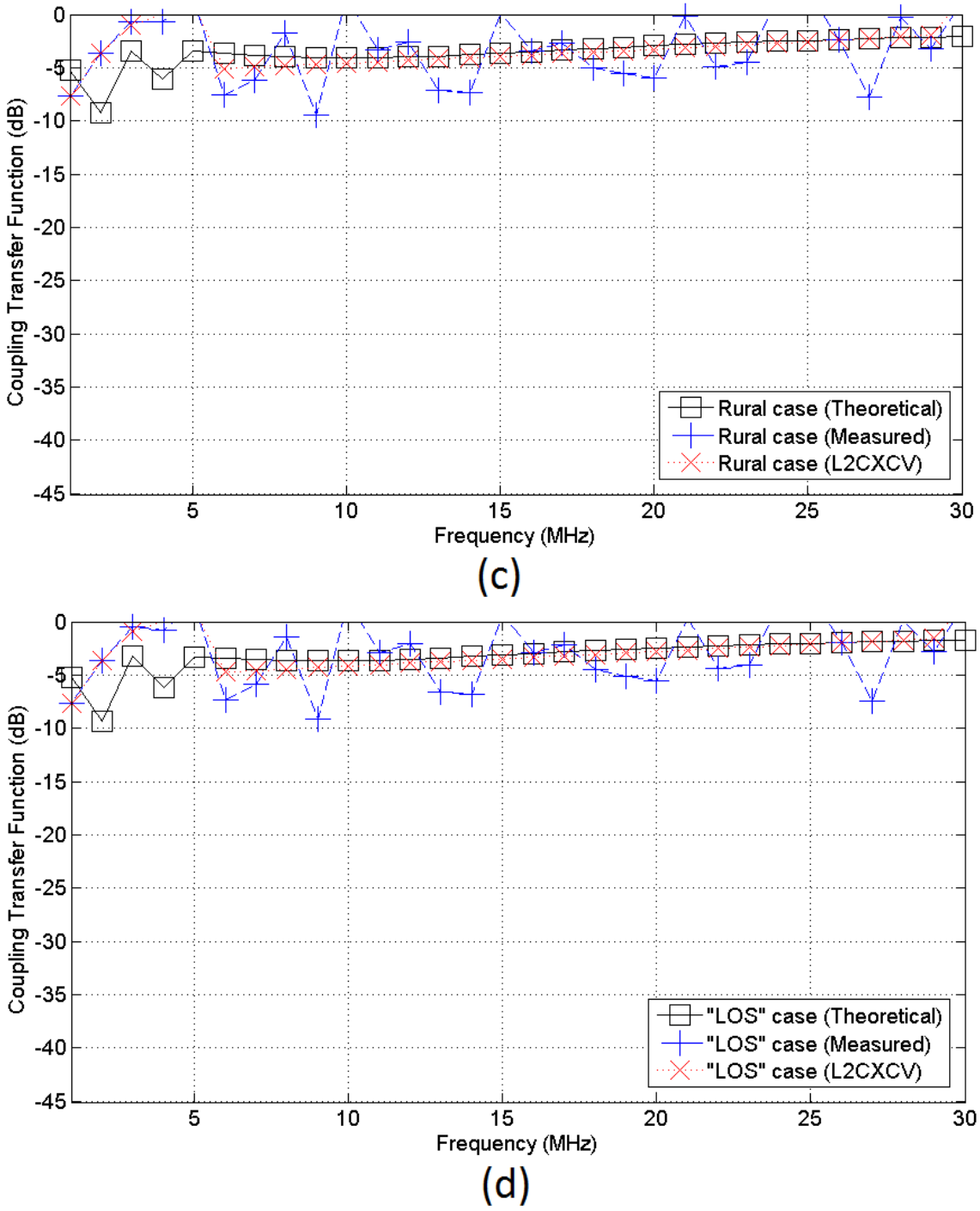

Figure 7. Same curves with Fig.2 but for L2CXCV.

From Figs. 5(a)-(d), 6(a)-(d), and 7(a)-(d), it is clearly demonstrated that all the examined piecewise monotonic data approximations are attempting to identify the primary extrema of the measured OV MV BPL transfer functions and, then, interpolate the coupling transfer function data at these extrema. In the case of L1PMA and L2WPMA, the low optimal number of monotonic sections poses restrictions so that high fluctuations due to the high magnitudes of measurement differences, which distort the

monotonicity pattern and exceed the optimal number of monotonic sections, can be mitigated. Hence, both L1PMA and L2WPMA very efficiently approximate the OV MV BPL coupling transfer functions of rural and "LOS" cases. However, when aggravated OV MV BPL topologies are examined (*e.g.*, urban and suburban case), the need for high number of monotonic sections is required so that the depth and the extent of spectral notches of the theoretical OV MV BPL coupling transfer function are successfully included. The high optimal number of monotonic sections gives sufficient freedom to fit the measured OV MV BPL coupling transfer function data without excluding measurement differences of high magnitude. Conversely, L2CXCV creates an average approximation that remains almost stable reducing the influence of gross measurement differences. Exploiting the CUD measurement difference nature, L2CXCV approximation generally follows the theoretical OV MV BPL coupling transfer functions in all the indicative OV MV BPL topologies examined.

To comparatively benchmark L1PMA, L2WPMA, and L2CXCV when measurement differences of different maximum CUD values occur, PES of each piecewise data approximation method as well as the PES_{fault} of indicative urban OV MV BPL topology are demonstrated in Table 2 when different maximum CUD values are applied. In Table 3, 4, and 5, same reports with Table 2 are presented but for the suburban, rural, and "LOS" case, respectively. Note that the optimal number of monotonic sections, which is presented in Table 1, is used for each indicative OV MV BPL topology.

TABLE 2
PES_{fault} and PES for the Indicative Urban OV MV BPL Topology when L1PMA, L2WPMA, and L2CXCV Are Applied for Different Maximum CUD Value

Maximum CUD Value (dB)	Urban Topology			
	PES_{fault} (%)	PES (%)		
		L1PMA	L2WPMA	L2CXCV
1	3.51	3.51	3.51	34.65
2	7.51	7.61	7.03	35.91
3	9.63	9.79	9.39	35.35
4	13.27	13.86	12.94	35.58
5	16.27	15.72	16.30	36.58
6	18.76	18.68	17.95	34.51
7	20.22	20.17	20.22	38.06
8	24.70	24.59	24.67	36.72
9	27.31	27.15	27.15	37.66
10	36.17	34.64	36.89	41.56

TABLE 3
PES_{fault} and PES for the Indicative Suburban OV MV BPL Topology when L1PMA, L2WPMA, and L2CXCV Are Applied for Different Maximum CUD Value

Maximum CUD Value (dB)	Suburban Topology			
	PES_{fault} (%)	PES (%)		
		L1PMA	L2WPMA	L2CXCV
1	5.74	5.74	5.74	36.77
2	12.27	12.27	12.27	36.71
3	15.74	15.74	15.74	36.21
4	21.69	21.69	21.69	37.46
5	26.61	26.56	25.13	38.27
6	30.68	30.68	30.68	36.01
7	33.07	33.07	33.07	40.07
8	40.39	40.39	40.39	39.78
9	44.66	44.66	44.66	40.60
10	59.14	59.14	59.14	58.34

TABLE 4
PES_{fault} and PES for the Indicative Rural OV MV BPL Topology when L1PMA, L2WPMA, and L2CXCV Are Applied for Different Maximum CUD Value

Maximum CUD Value (dB)	Rural Topology			
	PES_{fault} (%)	PES (%)		
		L1PMA	L2WPMA	L2CXCV
1	14.00	11.27	8.97	11.49
2	29.92	24.28	22.93	18.18
3	38.38	34.01	29.50	26.35
4	52.87	49.09	39.60	36.22
5	64.86	53.43	67.39	35.09
6	74.79	56.11	81.51	35.34
7	80.60	73.22	100.46	34.22
8	98.45	85.31	187.02	49.86
9	108.85	101.03	184.77	60.06
10	144.16	145.50	300.00	75.71

TABLE 5
PES_{fault} and PES for the Indicative "LOS" OV MV BPL Topology when
L1PMA, L2WPMA, and L2CXCV Are Applied for Different Maximum CUD Value

Maximum CUD Value (dB)	"LOS" Topology			
	PES_{fault} (%)	PES (%)		
		L1PMA	L2WPMA	L2CXCV
1	15.57	11.66	9.74	13.45
2	33.28	25.90	26.67	20.77
3	42.69	37.87	32.82	29.80
4	58.82	54.80	50.82	40.76
5	72.16	59.28	86.18	39.34
6	83.21	60.95	108.25	39.51
7	89.68	91.99	123.44	38.58
8	109.52	95.25	276.60	55.97
9	121.10	112.46	228.31	66.99
10	160.38	161.53	413.36	84.38

From Tables 2-5, a plethora of interesting conclusions can be revealed as follows:

- When the PES of a piecewise monotonic data approximation is lower than the respective PES_{fault} of the examined OV MV BPL topology for a given maximum CUD value, this implies that the approximated OV MV BPL coupling transfer function resembles more to the corresponding theoretical OV MV BPL transfer function than the measured one. Therefore, the mitigation of measurement differences may occur in the cases where the examined piecewise monotonic data approximations present lower PES than the corresponding PES_{fault}. Indeed, comparing PES_{fault} with PES of L1PMA, L2WPMA, and L2CXCV, at least one of the aforementioned piecewise monotonic data approximations achieves to mitigate the occurred measurement differences in 33 of the 40 cases examined, which is equivalent to 82.5%. Schematically, these 33 cases are illustrated with green background color in Tables 2-5.
- Further analyzing the cases where a measurement difference mitigation can be achieved, the following analytics can be pointed out:
    - L1PMA presents the best PES in 4 of the 33 examined cases, say 12.12%.
    - L2WPMA presents the best PES in 6 of the 33 examined cases, say 18.18%.
    - L2CXCV presents the best PES in 22 of the 33 examined cases, say 66.67%.
    - L1PMA and L2WPMA present the same best PES in 1 of the 33 examined cases, say 3.03%.
- Correlating the previous piecewise monotonic data approximation analytics with the examined OV MV BPL topologies, it is observed that:
    - During the OV MV BPL coupling transfer function approximation of topologies with low number of branches, such as "LOS" and rural cases, the spectral notches that observed in coupling transfer functions are

shallow and rare. Hence, OV MV BPL coupling transfer functions present wide ranges of flat spectral behavior while the optimal number of monotonic sections remains low. The measurement differences create fluctuations that can be counterbalanced by a simple approximation method, such as L2CXCV, that maintains a steady monotonicity pattern. Therefore, it is obvious that L2CXCV presents the best PES in comparison with L1PMA and L2WPMA when "LOS" and rural cases are examined.

- As the branch complexity of the OV MV BPL topologies raises so does the extent and the depth of spectral notches across the coupling transfer functions. Since an intense multipath environment is investigated, the need for including more primary and secondary extrema requires higher optimal number of monotonic sections. In these cases, the simple approximations, such as L2CXCV, fail to describe the richness of the notches cancelling the efficiency of these approximations. Here, L1PMA and L2WPMA are able to catch the complexity of the OV MV BPL coupling transfer functions. Indeed, L1PMA and L2WPMA can almost equivalently mitigate the measurement differences of the examined urban OV MV BPL topology.

- Relating the previous piecewise monotonic data approximation analytics with the different applied maximum CUD values, it can be pointed out that:
  - When the maximum CUD value remains low, *i.e.*, below 6-7dB, the measured OV MV BPL coupling transfer functions little differ from the theoretical ones due to the weak fluctuations. Based on the optimal number of monotonic sections, L1PMA and L2WPMA approximate the measured OV MV BPL coupling transfer functions near the theoretical one by omitting the weak fluctuations.
  - As the maximum CUD value increases, the measurement differences become important and comparable to the spectral notches of OV MV BPL coupling transfer functions. On the basis of the optimal number of monotonic sections, L1PMA and L2WPMA approximate the data through the prism of specific monotonic sections. Here, the high optimal number of monotonic sections may permit the overfit of L1PMA and L2WPMA during the approximations rendering unable the rejection of the extrema due to measurement differences. Conversely, L2CXCV produces a simple approximation, which tries to create an average fit neglecting the general fluctuations, that avoids the deficiency of the overfit of L1PMA and L2WPMA.

- To exploit the strong points of each of the aforementioned piecewise monotonic data approximations, an adaptive countermeasure technique against measurement differences should be proposed, as follows:
  - When the examined OV MV BPL topology is characterized by significant number of branches of short length (*i.e.*, urban topologies), L1PMA and L2WPMA should be adopted due to their proneness to easily adapt to the versatility of the coupling transfer functions of these topologies.
  - In contrast, when the examined OV MV BPL topologies consist of few long branches, a simple approximation, such as L2CXCV, is required to give an overall and more general picture of the measured OV MV BPL coupling transfer function. Since the theoretical OV MV BPL coupling

transfer functions present shallow spectral notches, their behavior is close to the approximation generated by the L2CXCV.

- The most crucial role during the comparative benchmarking of the previous piecewise monotonic data approximations plays the selection of the optimal number of monotonic sections. In fact, the optimal number of monotonic sections determines: (i) the accuracy of L1PMA and L2WPMA that is expressed by PES; and (ii) the result of the comparison between piecewise monotonic data approximations of monotonic sections (*e.g.*, L1PMA and L2WPMA) and the approximations without monotonic sections (*e.g.*, L2CXCV). Also, comparing PES results of this paper with those of [2], it is obvious that even if same OV BPL topologies are examined the PES results are differentiated because of the different applied coupling schemes and the optimal number of monotonic sections. Here, additional investigation should be made in order to clarify the impact of specific factors, such as the applied coupling scheme, the examined OV MV BPL topology, and maximum CUD value, on the optimal number of monotonic sections. Identifying this need for PES performance improvement of piecewise monotonic data approximations that are based on the number of monotonic sections, a detailed analysis of the influence of the previous factors on the PES performance of OV MV BPL topologies is given in the companion paper of [59].

Conclusions

In this paper, the performance of L1PMA, L2WPMA, and L2CXCV against the measurement differences, which can occur during the determination of OV MV BPL coupling transfer functions, has been assessed in terms of PES and PES_{fault}.

From the various PES comparisons among the examined piecewise monotonic data approximations and the measurement differences, it has been pointed out that the mitigation of measurement differences is possible in the vast majority of the OV MV BPL cases examined regardless of the occurred magnitudes of the measurement difference distributions. In fact, piecewise monotonic data approximations that are based on the optimal number of monotonic sections (*i.e.*, L1PMA and L2WPMA) better cope with the measurement differences in OV MV BPL topologies of intense multipath environments (*i.e.*, urban topologies) whereas piecewise monotonic data approximations without monotonic sections better deal with the measurement differences of OV MV BPL topologies of "quiet" multipath environments (*i.e.*, suburban, rural, and "LOS" topologies). Depending on the examined OV MV BPL topology, a versatile measurement difference mitigation technique, which is going to use: (i) L2CXCV for the rural and "LOS" cases; and (ii) L1PMA or L2WPMA for the suburban and urban cases; could exploit all the 82.5% potential of mitigating measurement differences.

However, L1PMA and L2WPMA may further be enhanced if the selection of the optimal number of monotonic sections is further studied. The companion paper of [59] strengthens the PES efficiency of L1PMA and L2WPMA of this paper.

Conflicts of Interest

The author declares that there is no conflict of interests regarding the publication of this paper.

References

[1] K. Ali, I. Pefkianakis, A. X. Liu, and K. H. Kim, "Boosting PLC Networks for High-Speed Ubiquitous Connectivity in Enterprises," arXiv preprint arXiv:1608.06574, 2016, [Online]. Available: http://arxiv.org/pdf/1608.06574v1.pdf (Accessed on 11/25/2016)

[2] A. G. Lazaropoulos, "Best L1 Piecewise Monotonic Data Approximation in Overhead and Underground Medium-Voltage and Low-Voltage Broadband over Power Lines Networks: Theoretical and Practical Transfer Function Determination," *Hindawi Journal of Computational Engineering*, vol. 2016, Article ID 6762390, 24 pages, 2016. DOI: 10.1155/2016/6762390.

[3] C. Cano, A. Pittolo, D. Malone, L. Lampe, A. M.Tonello, and A. Dabak, "State-of-the-art in Power Line Communications: From the Applications to the Medium," *IEEE J. Sel. Areas Commun.*,vol. 34, pp. 1935-1952, 2016.

[4] L. Lampe, A. M. Tonello, and T. G. Swart, *Power Line Communications: Principles, Standards and Applications from Multimedia to Smart Grid*. John Wiley & Sons, 2016.

[5] Homeplug, Technology Gains Momentum, 2013, [Online]. Available: http://www.businesswire.com (Accessed on 11/25/2016)

[6] Homeplug, AVWhitepaper, 2007, [Online]. Available: http://www.homeplug.org/techresources/resources/ (Accessed on 11/25/2016)

[7] Homeplug, AV2Whitepaper, 2011, [Online]. Available: http://www.homeplug.org/techresources/resources/ (Accessed on 11/25/2016)

[8] A. G. Lazaropoulos and P. G. Cottis, "Transmission characteristics of overhead medium voltage power line communication channels," *IEEE Trans. Power Del.*, vol. 24, no. 3, pp. 1164-1173, Jul. 2009.

[9] A. G. Lazaropoulos and P. G. Cottis, "Capacity of overhead medium voltage power line communication channels," *IEEE Trans. Power Del.*, vol. 25, no. 2, pp. 723-733, Apr. 2010.

[10] A. G. Lazaropoulos and P. G. Cottis, "Broadband transmission via underground medium-voltage power lines-Part I: transmission characteristics," *IEEE Trans. Power Del.*, vol. 25, no. 4, pp. 2414-2424, Oct. 2010.

[11] A. G. Lazaropoulos and P. G. Cottis, "Broadband transmission via underground medium-voltage power lines-Part II: capacity," *IEEE Trans. Power Del.*, vol. 25, no. 4, pp. 2425-2434, Oct. 2010.

[12] A. G. Lazaropoulos, "Broadband transmission characteristics of overhead high-voltage power line communication channels," *Progress in Electromagnetics Research B*, vol. 36, pp. 373-398, 2012. DOI: 10.2528/PIERB11091408

[13] A. G. Lazaropoulos, "Capacity Performance of Overhead Transmission Multiple-Input Multiple-Output Broadband over Power Lines Networks: The Insidious Effect of Noise and the Role of Noise Models," *Trends in Renewable Energy*, vol. 2, no. 2, pp. 61-82, Jan. 2016. DOI: 10.17737/tre.2016.2.2.0023

[14] A. G. Lazaropoulos, "Factors Influencing Broadband Transmission Characteristics of Underground Low-Voltage Distribution Networks," *IET Commun.*, vol. 6, no. 17, pp. 2886-2893, Nov. 2012.

[15] A. G. Lazaropoulos, "Towards broadband over power lines systems integration: Transmission characteristics of underground low-voltage distribution power lines," *Progress in Electromagnetics Research B*, 39, pp. 89-114, 2012. DOI: 10.2528/PIERB12012409

[16] A. G. Lazaropoulos, "Broadband transmission and statistical performance properties of overhead high-voltage transmission networks," *Hindawi Journal of Computer Networks and Commun.*, 2012, article ID 875632, 2012. DOI: 10.1155/2012/875632

[17] A. G. Lazaropoulos, "Towards modal integration of overhead and underground low-voltage and medium-voltage power line communication channels in the smart grid landscape: model expansion, broadband signal transmission characteristics, and statistical performance metrics (Invited Paper)," *ISRN Signal Processing*, vol. 2012, Article ID 121628, 17 pages, 2012. DOI: 10.5402/2012/121628

[18] A. G. Lazaropoulos, "Review and Progress towards the Common Broadband Management of High-Voltage Transmission Grids: Model Expansion and Comparative Modal Analysis," *ISRN Electronics*, vol. 2012, Article ID 935286, pp. 1-18, 2012. DOI: 10.5402/2012/935286

[19] A. G. Lazaropoulos, "Review and Progress towards the Capacity Boost of Overhead and Underground Medium-Voltage and Low-Voltage Broadband over Power Lines Networks: Cooperative Communications through Two- and Three-Hop Repeater Systems," *ISRN Electronics*, vol. 2013, Article ID 472190, pp. 1-19, 2013. DOI: 10.1155/2013/472190

[20] A. G. Lazaropoulos, "Green Overhead and Underground Multiple-Input Multiple-Output Medium Voltage Broadband over Power Lines Networks: Energy-Efficient Power Control," *Journal of Global Optimization*, vol. 57, no. 3, pp 997–1024, Nov. 2013. DOI: 10.1007/s10898-012-9988-y

[21] P. Amirshahi and M. Kavehrad, "High-frequency characteristics of overhead multiconductor power lines for broadband communications," *IEEE J. Sel. Areas Commun.*, vol. 24, no. 7, pp. 1292-1303, Jul. 2006.

[22] T. Sartenaer, "Multiuser communications over frequency selective wired channels and applications to the powerline access network" Ph.D. dissertation, Univ. Catholique Louvain, Louvain-la-Neuve, Belgium, Sep. 2004.

[23] T. Calliacoudas and F. Issa, ""Multiconductor transmission lines and cables solver," An efficient simulation tool for plc channel networks development," presented at the *IEEE Int. Conf. Power Line Communications and Its Applications*, Athens, Greece, Mar. 2002.

[24] A. G. Lazaropoulos, "Measurement Differences, Faults and Instabilities in Intelligent Energy Systems –Part 1: Identification of Overhead High-Voltage Broadband over Power Lines Network Topologies by Applying Topology Identification Methodology (TIM)," *Trends in Renewable Energy*, vol. 2, no. 3, pp. 85 – 112, Oct. 2016. DOI: 10.17737/tre.2016.2.3.0026

[25] A. G. Lazaropoulos, "Measurement Differences, Faults and Instabilities in Intelligent Energy Systems – Part 2: Fault and Instability Prediction in Overhead High-Voltage Broadband over Power Lines Networks by Applying Fault and Instability Identification Methodology (FIIM)," *Trends in Renewable Energy*, vol. 2, no. 3, pp. 113 – 142, Oct. 2016. DOI: 10.17737/tre.2016.2.3.0027

[26] I. C. Demetriou and M. J. D. Powell, "Least squares smoothing of univariate data to achieve piecewise monotonicity," *IMA J. of Numerical Analysis*, vol. 11, pp. 411-432, 1991.

[27] I. C. Demetriou and V. Koutoulidis, "On Signal Restoration by Piecewise Monotonic Approximation", in Lecture Notes in Engineering and Computer

Science: *Proceedings of The World Congress on Engineering 2013*, London, U.K., Jul. 2013, pp. 268-273.

[28] I. C. Demetriou, "An application of best *L*1 piecewise monotonic data approximation to signal restoration," *IAENG International Journal of Applied Mathematics*, vol. 53, no. 4, pp. 226-232, 2013.

[29] I. C. Demetriou, "L1PMA: A Fortran 77 Package for Best L1 Piecewise Monotonic Data Smoothing," *Computer Physics Communications*, vol. 151, no. 1, pp. 315-338, 2003.

[30] I. C. Demetriou, "Data Smoothing by Piecewise Monotonic Divided Differences," *Ph.D. Dissertation*, Department of Applied Mathematics and Theoretical Physics, University of Cambridge, Cambridge, 1985.

[31] I. C. Demetriou, "Best L1 Piecewise Monotonic Data Modelling,"*Int. Trans. Opl Res.*, vol. 1, no. 1, pp. 85-94,1994.

[32] C. de Boor, *A Practical Guide to Splines*. Revised Edition, NY: Springer-Verlag, Applied Mathematical Sciences, vol. 27, 2001.

[33] M. Holschneider, *Wavelets. An Analysis Tool*, Oxford: Clarendon Press, 1997.

[34] I. C. Demetriou, "Algorithm 863: L2WPMA, a Fortran 77 package for weighted least-squares piecewise monotonic data approximation," *ACM Transactions on Mathematical Software (TOMS)*, vol. 33, no.1, pp. 6, 2007.

[35] I. C. Demetriou, "L2CXCV: A Fortran 77 package for least squares convex/concave data smoothing," *Computer physics communications*, vol. 174, no.8, pp. 643-668, 2006.

[36] P. Amirshahi, "Broadband access and home networking through powerline networks" Ph.D. dissertation, Pennsylvania State Univ., University Park, PA, May 2006. [Online]. Available: http://etda.libraries.psu.edu/theses/approved/WorldWideIndex/ETD-1205/index.html (Accessed on 11/25/2016)

[37] M. D'Amore and M. S. Sarto, "Simulation models of a dissipative transmission line above a lossy ground for a wide-frequency range-Part I: Single conductor configuration," *IEEE Trans. Electromagn. Compat.*, vol. 38, no. 2, pp. 127-138, May 1996.

[38] M. D'Amore and M. S. Sarto, "Simulation models of a dissipative transmission line above a lossy ground for a wide-frequency range-Part II: Multi-conductor configuration," *IEEE Trans. Electromagn. Compat.*, vol. 38, no. 2, pp. 139-149, May 1996.

[39] A. Milioudis, G. T. Andreou, and D. P. Labridis, "Detection and location of high impedance faults in multiconductor overhead distribution lines using power line communication devices," *IEEE Trans. on Smart Grid*, vol. 6, no. 2, pp. 894-902, 2015.

[40] A. G. Lazaropoulos, "Designing Broadband over Power Lines Networks Using the Techno-Economic Pedagogical (TEP) Method – Part I: Overhead High Voltage Networks and Their Capacity Characteristics," *Trends in Renewable Energy*, vol. 1, no. 1, pp. 16-42, Mar. 2015. DOI: 10.17737/tre.2015.1.1.002

[41] A. G. Lazaropoulos, "Designing Broadband over Power Lines Networks Using the Techno-Economic Pedagogical (TEP) Method – Part II: Overhead Low-Voltage and Medium-Voltage Channels and Their Modal Transmission Characteristics," *Trends in Renewable Energy*, vol. 1, no. 2, pp. 59-86, Jun. 2015. DOI: 10.17737/tre.2015.1.2.006

[42] T. Sartenaer and P. Delogne, "Deterministic modelling of the (Shielded) outdoor powerline channel based on the multiconductor transmission line equations," *IEEE J. Sel. Areas Commun.*, vol. 24, no. 7, pp. 1277-1291, Jul. 2006.

[43] OPERA1, D5: Pathloss as a function of frequency, distance and network topology for various LV and MV European powerline networks. IST Integrated Project No 507667, Apr. 2005.

[44] OPERA1, D44: Report presenting the architecture of plc system, the electricity network topologies, the operating modes and the equipment over which PLC access system will be installed, IST Integr. Project No 507667, Dec. 2005.

[45] A. G. Lazaropoulos, "The Impact of Noise Models on Capacity Performance of Distribution Broadband over Power Lines (BPL) Networks," *Hindawi Computer Networks and Communications*, vol. 2016, Article ID 5680850, 14 pages, 2016. DOI: 10.1155/2016/5680850.

[46] A. G. Lazaropoulos, "Policies for Carbon Energy Footprint Reduction of Overhead Multiple-Input Multiple-Output High Voltage Broadband over Power Lines Networks," *Trends in Renewable Energy*, vol. 1, no. 2, pp. 87-118, Jun. 2015. DOI: 10.17737/tre.2015.1.2.0011

[47] A. G. Lazaropoulos, "Wireless Sensor Network Design for Transmission Line Monitoring, Metering and Controlling: Introducing Broadband over PowerLines-enhanced Network Model (BPLeNM)," *ISRN Power Engineering*, vol. 2014, Article ID 894628, 22 pages, 2014. DOI: 10.1155/2014/894628.

[48] A. G. Lazaropoulos, "Wireless Sensors and Broadband over PowerLines Networks: The Performance of Broadband over PowerLines-enhanced Network Model (BPLeNM) (Invited Paper)," *ICAS Publishing Group Transaction on IoT and Cloud Computing*, vol. 2, no. 3, pp. 1-35, 2014.

[49] M. J. D. Powell, *Approximation Theory and Methods*. Cambridge, U.K.: Cambridge University Press, 1981.

[50] A. G. Lazaropoulos, *Engineering the Art through the Lens of L1PMA: A Tribute to the Modern Greek Painters*, Art Book ISSUU Digital Publishing Platform, Oct. 2014. [Online]. Available: http://issuu.com/lazaropoulos/docs/l1pma (Accessed on 11/25/2016)

[51] A. G. Lazaropoulos, *ReEngineering the Art through the Lens of L2WPMA: A Tribute to Leonardo da Vinci's Inventions: Flying Machines, War Machines, Architect/Innovations and Water Land Machines*, Art Book ISSUU Digital Publishing Platform, Nov. 2014. [Online]. Available: http://issuu.com/lazaropoulos/docs/l2wpma (Accessed on 11/25/2016)

[52] A. G. Lazaropoulos, *ReEngineering the Art through the Lens of L1PMA L2WPMA: The Eternal Youth of the Parthenon Art, Architecture, Marble Sculpture, Metallurgy Pottery*, Art Book ISSUU Digital Publishing Platform, Dec. 2014. [Online]. Available: http://issuu.com/lazaropoulos/docs/l1pma_l2wpma (Accessed on 11/25/2016)

[53] http://cpc.cs.qub.ac.uk/summaries/ADRF (Accessed on 11/25/2016)

[54] http://www.cpc.cs.qub.ac.uk/summaries/ADXM_v1_0.html (Accessed on 11/25/2016)

[55] T. Banwell and S. Galli, "A novel approach to accurate modeling of the indoor power line channel—Part I: Circuit analysis and companion model," *IEEE Trans. Power Del.*, vol. 20, no. 2, pp. 655-663, Apr. 2005.

[56] S. Galli and T. Banwell, "A novel approach to accurate modeling of the indoor power line channel — Part II: Transfer function and channel properties," *IEEE Trans. Power Del.*, vol. 20, no. 3, pp. 1869-1878, Jul. 2005.

[57] S. Galli and T. Banwell, "A deterministic frequency-domain model for the indoor power line transfer function," *IEEE J. Sel. Areas Commun.*, vol. 24, no. 7, pp. 1304-1316, Jul. 2006.

[58] A. G. Lazaropoulos, "Deployment Concepts for Overhead High Voltage Broadband over Power Lines Connections with Two-Hop Repeater System: Capacity Countermeasures against Aggravated Topologies and High Noise Environments," *Progress in Electromagnetics Research B*, vol. 44, pp. 283-307, 2012. DOI: 10.2528/PIERB12081104

[59] A. G. Lazaropoulos, "Power Systems Stability through Piecewise Monotonic Data Approximations – Part 2: Adaptive Number of Monotonic Sections and Performance of L1PMA, L2WPMA, and L2CXCV in Overhead Medium-Voltage Broadband over Power Lines Networks," *Trends in Renewable Energy*, vol. 3, no. 1, 33-60, Jan. 2017. DOI: 10.17737/tre.2017.3.1.0030